# Discrimination between facies and global controls in isotope composition of carbonates: carbon and oxygen isotopes at the Devonian reef margin in Moravia (HV-105 Křtiny borehole)

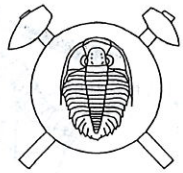

## Rozlišení faciálních a globálních vlivů v izotopovém složení karbonátů: izotopy uhlíku a kyslíku na čelním okraji devonského útesového komplexu na Moravě (vrt Křtiny HV-105) (Czech summary)

*(7 text-figs.)*

JANA HLADÍKOVÁ[1] - JINDŘICH HLADIL[2] - JAROSLAVA ZUSKOVÁ[1]

[1]*Geological Survey, Klárov 3, 118 21 Praha 1, Czech Republic*
[2]*Geological Institute AS CR, Rozvojová 135, 165 02 Praha 6, Czech Republic*

Relations among the isotope ratios, chemical composition, sedimentological features, eustatic fluctuations and diagenetical history have been documented from the reef/basin transition in the Moravian Karst (Křtiny HV-105 borehole). The $\delta^{13}C$ and $\delta^{18}O$ values of the Late Devonian limestones are within the ranges for the Late Devonian marine sedimentary environment. Nevertheless, the originally diverse isotopic compositions of the fossils and other rock components were changed in closed marine pore-water/rock systems, under conditions of rapidly decreased permeability. In the studied sequence $\delta^{13}C$ values of 2 to 2.5 ‰ are characteristic for bioherms, parts of the fore-reef to off-reef slope, and off-shore lagoons. The $\delta^{13}C$ values close to 0 ‰ are characteristic for shallow back-reef. The low $\delta^{13}C$ values of reef margin developed during the occasional emergence of this facies. A significant anomaly in $\delta^{13}C$ values (up to +5.5 ‰) has been documented at the transition between the proximal and distal forereef in the *Pa. transitans* Zone of the Early Frasnian, just before the maximum sea-level rise. This unusual positive excursion of the $\delta^{13}C$ values does not correspond to the global-event anomalies. The existence of this anomaly on the slope of the Moravian Karst is tentatively explained by a local III$^{rd}$-category upwelling, a result of the diversion of the deeper contour and shallower wind-driven currents away from the shore. This anomaly corroborates the hypothesis of a strong facies control of the $^{13}C$ content in carbonates.

*Key words*: Late Devonian, carbon and oxygen isotopes, geochemistry, diagenesis, sedimentary environment, sea-level changes, conodont stratigraphy, sequence stratigraphy, reef complexes, Moravia

The full-cored water-survey well HV-105 was drilled on the eastern margin of the Moravian Karst, 0.6 km SE of the Křtiny Church (Taraba 1976). Depth of the borehole was 0.5 km. Position of this borehole within the almost tectonically undisturbed reef/basin transition enabled us to find larger spectrum of the facies than on the platform (Hladil 1983, Dvořák et al. 1984). We assume that the diversity of facies on this transition yields better chance for the discrimination between the global and local controls in the isotope composition.

The Late Devonian carbonates of the HV-105 borehole were deposited on the margin of carbonate platforms which rimmed the Laurussia continent on the southeast. The palaeomagnetic estimates of palaeolatitudes are 14 to 12° South (Krs et al. 1995). The sediments of the platforms are mostly dark-grey with an unusually high amount of micrite which was massively precipitated by blue-green algae. These features correspond to very hot climate. Two features are typical for the late diagenesis of the rocks: a uniform fine recrystallisation of the rock and the high maximum temperatures of about 350 °C (CAI - changes of colour of conodonts, organic matter and magnetomineralogy; Krs et al. 1995). The both features indicate the deep burial conditions under the load of Culm formations and nappe stacks.

## HV-105 Křtiny well: reviewed and updated outline of the drilled sedimentary sequences

Below several meters of Quaternary river sediment (0-11.5 m), first 60 m of hard-rock was drilled in siliciclastics of the Viséan Culm facies. Lack of erosion bed or pebbly accumulations characterises the base of the Culm in this section. Scattered turbidite banks consist of medium- to fine-grained, quartz-rich graywacke which contrasts with the prevailing silty-clayey sediments. Dark, fine-laminated siltstone of distal turbidite origin dominates and its calculated $Al_2O_3/Na_2O$ ratio is low (<14; see Dvořák et al. 1984). The lowermost 10 m of the Viséan siliciclastic formation strongly differ from the overlying diastrophic and highstand sedimentation by the presence of oxygenated organic matter and iron. This basal layer consists of well-matured, silty and sandy shale which displays a very high $Al_2O_3/Na_2O$ ratio (>128; Dvořák et al. 1984). This depositional period has been correlated with the late Tournaissian/early Viséan lowstand when big karstified islands were rounded by marshes with dense vegetation. Estimates of the age are based on the palaeontological correlation with the entire region of the Moravian Karst (Lower/Middle Viséan trilobites, and *Sc. anchoralis* conodonts of terminating Tournaissian; I. Chlupáč, Z. Krejčí - personal communication 1995). No age determination from the drilled core is available.

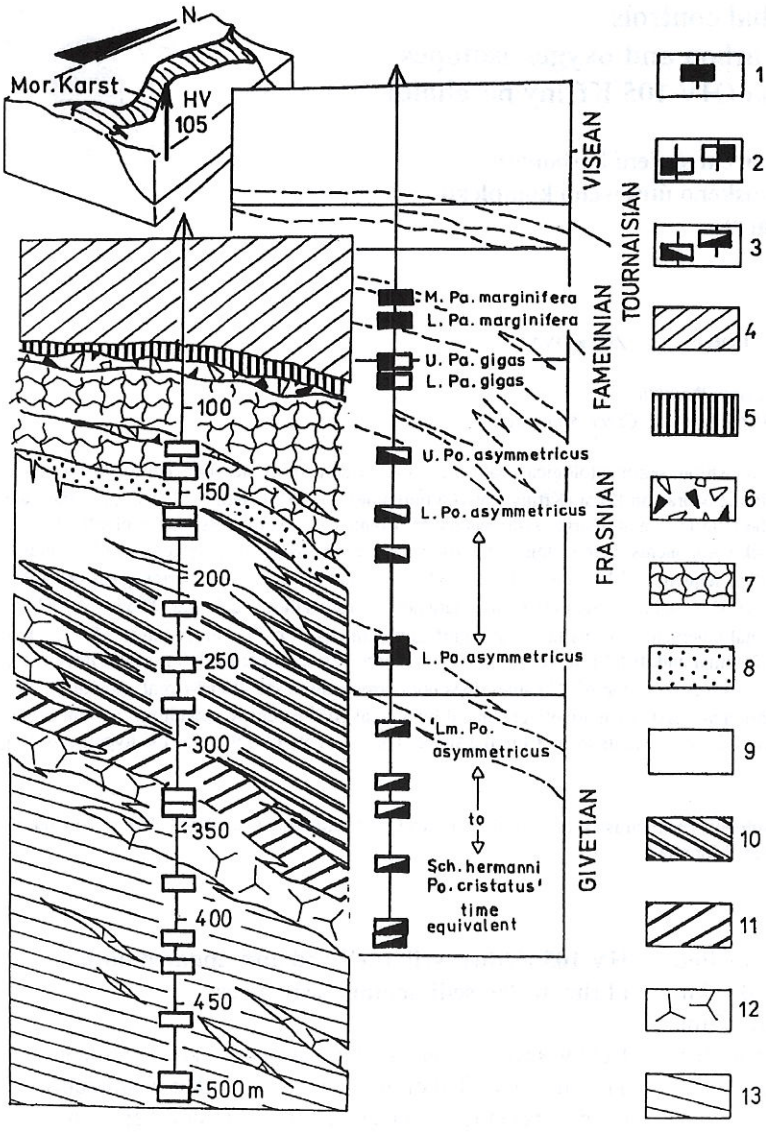


Fig. 1. Isotope samples from the Křtiny HV-105 borehole: depth in the borehole, facies and their age
Symbols for the samples (main carbonate facies): 1 - nodular limestone; 2 - reef cap (left), reef margin (right); 3 - fore reef (left), back reef (right). Formal lithostratigraphic units (drilled section): 4 - Protivanov Formation, Rozstání Member; 5 - Moravský Beroun Formation, Březina Shale; 6 - Moravský Beroun Formation, Hostěnice Breccia; 7 - Líšeň Formation, Křtiny Limestone; 8, 9 and 11 - Macocha Formation, Vilémovice Limestone; 10 - Macocha Formation, Vintoky Member; 12 and 13 - Macocha Formation, Lažánky Limestone. Lithology and age: 4 - silty shale with graywacke (diastrophic sedimentation, Late Viséan); 5 - carbonaceous silty red shale (mature sediment, latest Tournaissian - Early/Middle Viséan; 6 - carbonate breccia (Tournaissian); 7 - lime mudstone cover of the extinct reef (Late Famennian - Tournaisian); 8 - carbonate ramp, packstone/grainstone and rudstone/bindstone (Early Famennian); 9 - reef cap, boundstone/biocementstone and rudstone (Late Frasnian); 10 - fore reef, off reef, fine grained calciturbidite banks alternating the clayey sedimentary background (Middle Frasnian); 11 - cover of drowned reef, clayey wackestone/packstone with nodular structure (terminating Early Frasnian); 12 - reef margin, boundstone, chasms and seams filled by rudstone (Early Frasnian); 13 - back reef, packstone/floatstone and packstone/bafflestone, mostly Amphipora-beds (beginning Early Frasnian)

In contrast, the uppermost parts of the drilled carbonate complex consist of offshore sediments: an upward thinning and fining sequence consists of calciturbidites and nodular limestones. Debris-flows with phosphate cherts are within the uppermost part of the sequence (Fig. 1). Major debris-flows have been correlated with the late Middle Tournaissian. Another level is embedded in late *Pa. marginifera* nodular limestone, cf. Habrůvka site in the neighbourhood, but this level has been weakly documented in the drilled section. This non-reef limestone formation ranges from Tournaisian down to the Famennian, its base is marked by a thin layer with *Pa. rhomboidea* conodont fauna (the Devonian-Carboniferous boundary is at 88.8 m; the base of the formation at 144.6 m). An increased rate of the calciturbidite deposition was documented in *Pa. marginifera* Zone (130.0-143.0 m) where the limestone banks alternate the clayey layers; the clayey and silty material displays moderately high $Al_2O_3/Na_2O$ ratios (>50; Dvořák et al. 1984). Upwelling of deep oceanic water associated with oversaturation in abiotic nutrients can explain the depletion of the benthos up to the proximal slope. This upwelling probably reflected the low sea-level of Famennian times when majority of former proximal carbonate shelves was emerged (mixed ocean water). Transition to Early Famennian lithological type is recorded within 1.6 m of the drilled core.

The Early Famennian sediments (depth 144.6-159.5 m) are mostly medium to light-grey tempestites, rarely they consist of sliding portions of sediments in conditions of proximal-slope. Some thicker portions were amalgamated, but the thinner beds in slabs display cross-bedding. Mud-supported structure of grainstone involves bio- and lithoclasts. Micritisation, "chalkification" and "tarnish-clouded" alterations on some grains indicate the vadose diagenesis on some rock particles before the final resedimentation. An enormous number of algal and larval spheres are accompanied by tiny debris of brachiopods, coralline algae, crinoids, echinoids, and bryozoans. Thick-walled podocopid ostracod shells are abundant. Corals and stromatoporoids are scattered, usually in fragments; they are starving colonies with many malformations and injuries caused by transported clasts or browsing grazers. This type of sediments ran-

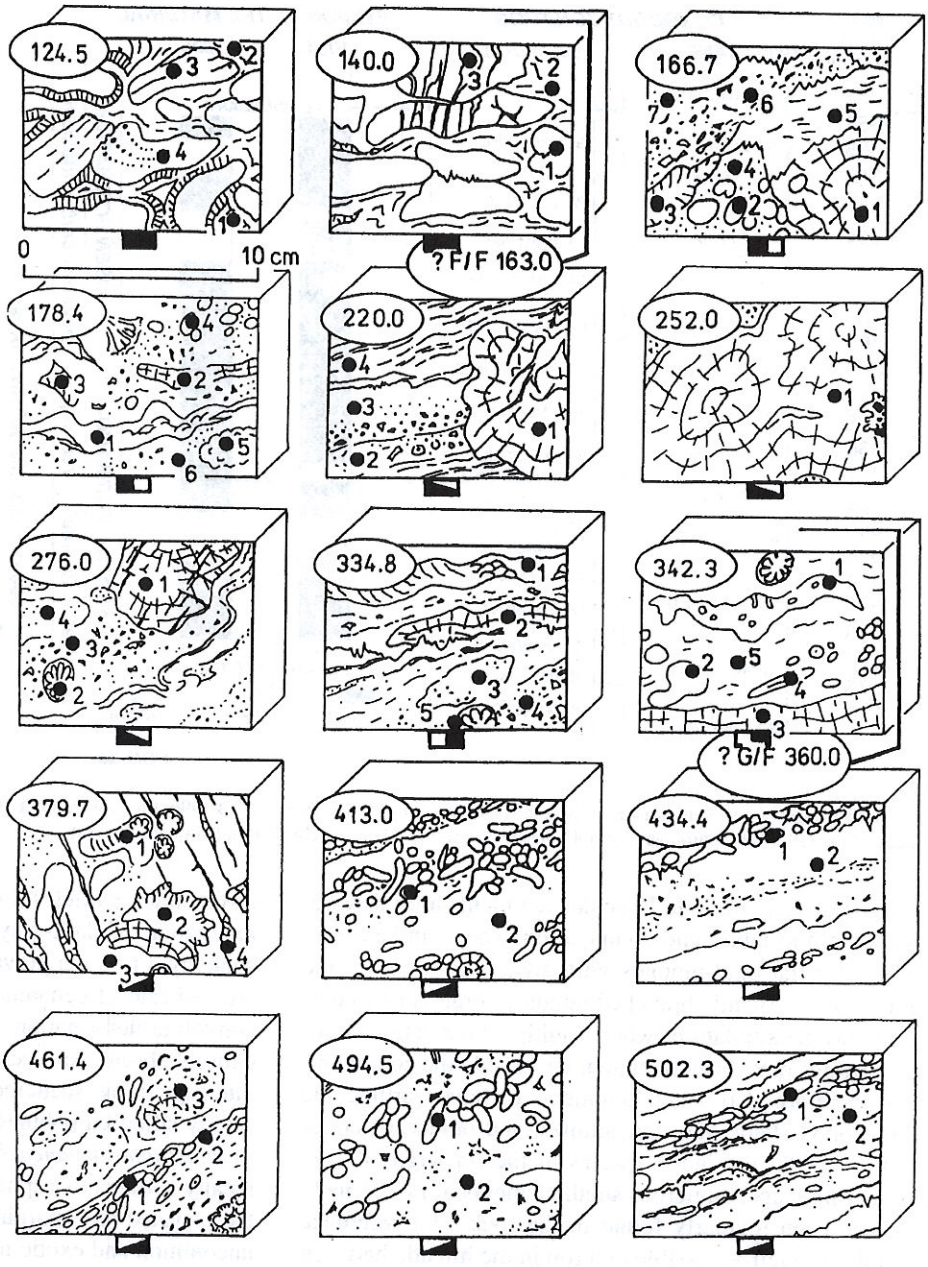


Fig. 2. Core slabs sampled for isotope analysis, in detail: relation to the structure of the rocks. 124.5 m: 1 - zonal marine cement in open structures among the nodules washed out from the semi-lithified sediment (dirty white); 2 - lime-mud matrix (yellowish grey); 3 - a nodule of laminated wackestone (grey); 4 - a nodule of intraclastic packstone, porous (reddish grey). 140.0 m: 1 - massive wackestone in a nodule (grey); 2 - lime mudstone in matrix (brownish grey); 3 - calcite veins in a fractured nodule (white). 166.7 m: 1 - coenosteum of *Actinostroma tabulatum* (medium grey); 2 - coenosteum of *Stachyodes lagowiensis* (light grey); 3 - corallum of *Scoliopora denticulata* (medium grey); 4 - rock matrix, fine-grained and well-sorted stachyodid debris (light grey); 5 - rock matrix, lime mudstone with scattered lithoclastic grains (medium grey); 6 - rock matrix, unsorted debris of different bioclastic components (medium to light grey); 7 - an ultra-fine carbonate silt layer, deposited reef milk (medium grey). 178.4 m: 1 - corallum of *Alveolites complanatus* (light grey); 2 - coenosteum of *Actinostroma devonense* (medium grey); 3 - corallum of *Scoliopora kaisini* (light grey); 4 - coenosteum of *Stachyodes regularis* (light grey); 5 - an alga, undetermined (white); 6 - rock matrix, fine-grained, sorted bioclastic grainstone with rounded grains (light grey). 220.0 m: 1 - a redeposited coenosteum fragment of *Actinostroma tabulatum* (dark grey); 2 - crinoidal packstone (medium grey); 3 - lithoclastic packstone, graded bedding (medium grey); 4 - lime mudstone and wackestone/microbioclastic calcisiltite (dark to medium grey). 252.0 m: 1 - a redeposited head-pebble of Actinostroma tabulatum (dark grey). 276.0 m: 1 - fragment of A. tabulatum, organic matter in densely spaced fractures, slight silicification (dark grey); 2 - rugose coral *Temnophyllum* sp., a fragment (light grey); 3 - packstone with poorly sorted bioclasts and lithoclasts (dark grey); 4 - a nodule originated from a layer of massive calcisiltite (dark to medium grey). 334.8 m: 1 - corallum of *Alveolites delhayei* (medium to light grey); 2 - fragment of a coenosteum of *Hermatostroma* sp. (light grey); 3 - clast of formerly semi-solid bioclastic packstone/grainstone, fine and sorted grains (light grey); 4 - rock matrix, grainstone with different kind and size of bioclasts (light grey); 5 - a fragment of rugose coral *Thamnophyllum monozonatum* (light grey). 342.3 m: 1 - coenosteum of *Clathrocoilona* sp. (dirty white); 2 - corallum fragments of *Thamnopora boloniensis* (white); 3 - top of a cube head of *Hermatostroma polymorphum* (light grey); 4 - a pencil-like coenosteum of *Amphipora laxeperforata* (light grey); 5 - rock matrix, packstone/grainstone (medium to light grey). 379.7 m: 1 - rugose coral *Disphyllum regulare* (dirty white); 2 - corallum of *Alveolites mailleuxi* (medium grey); 3 - massive biocementstone (medium grey); 4 - carbonate veins in early fractured rock (dirty white). 413.0 m: 1 - stem of *Amphipora rudis* (medium to light grey); 2 - rock matrix, packstone with abundant green-alga tubes, Issinella sp. (dark grey). 434.4 m: 1 - stem of *Amphipora pinguis* (medium grey); 2 - rock matrix, packstone with lithoclasts and bioclasts, scattered micritised and pyritised grains (dark grey). 461.4 m: 1 - a distorted coenosteum of *Amphipora angusta* (medium grey); 2 - rock matrix, bioclastic packstone with debris of amphiporids, algae and gastropods (dark grey); 3 - formerly a semi-solid lithoclast, consisting of poorly washed grainstone with fragments of stromatoporoids (medium grey). 494.5 m: 1 - stem of *Amphipora angusta* (medium grey); 2 - rock matrix, recrystallised wackestone with scattered algal tubes (dark grey). 502.3 m: 1 - stem of *Amphipora angusta* (medium grey); 2 - rock matrix, packstone with chips of amphiporid tissues and fine debris of brachiopod shells, numerous solution sutures (dark brownish grey)

ges from the *Pa. crepida* down to the Late *Pa. triangularis* Zone. The underlying dark interval, between 159.5 and 162.3 m, contains a condensed sedimentary record where increased amount of micrite is typical, but numerous hardground surfaces and thin intercalations of lags reflect the sedimentary condensation. Age of these dark beds corresponds to Early *Pa. triangularis* Z. and particularly to the Upper Kellwasser Event (cf. McGhee 1986).

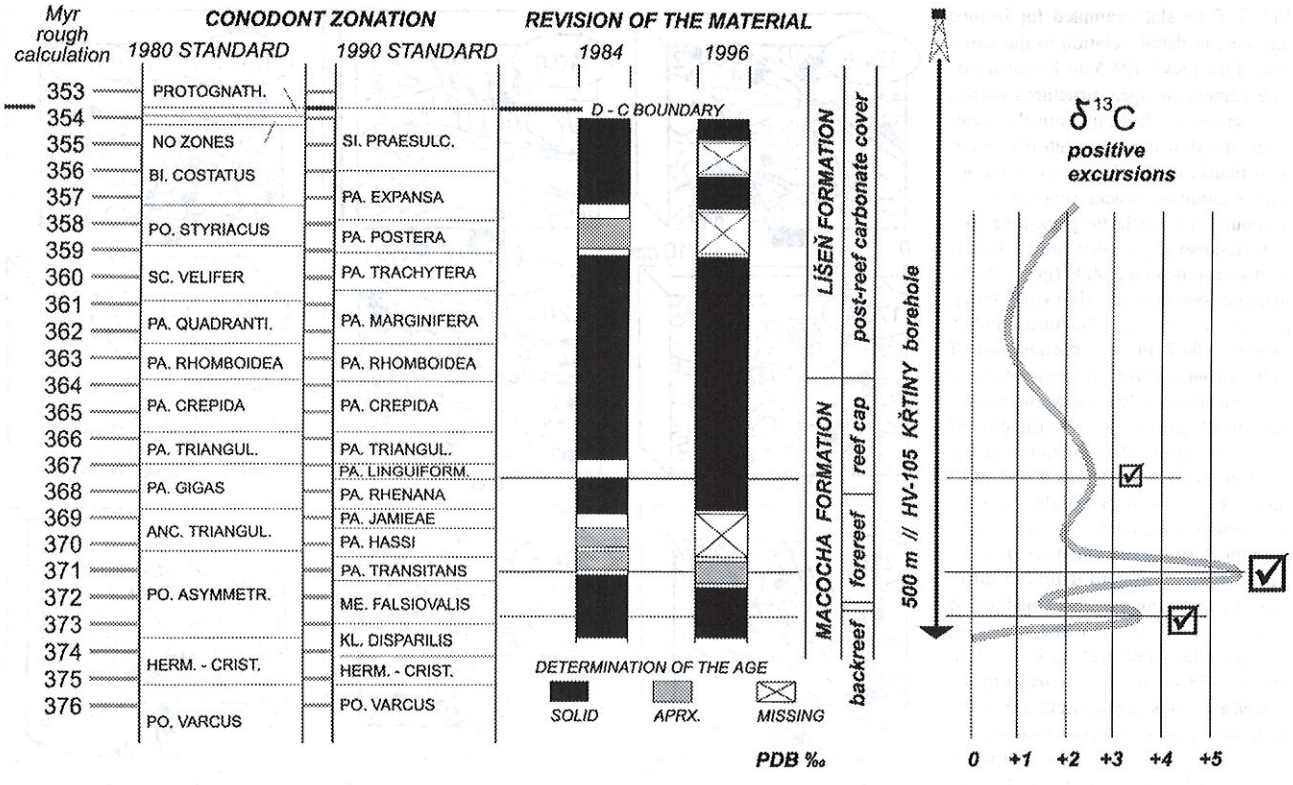


Fig. 3. Conodont zones: comparison of the zones and their application in 1984 and 1996; time assignment of the positive the $\delta^{13}C$ anomalies. An approach of the GSA 1990 chronostratigraphy has been used for the time correlation [Ma], see the text

The underlying Late Frasnian sediments are fairly variable both in fabric and composition. They can be exemplified by flat mud-mounds with algae, scolioporids and graciloporids (gentle branched tabulate corals) or by coarse pebbly accumulations where multiple brecciation or coral coatings have been documented. Beside the coral benthos, there are also pelagic elements of fauna: orthoconic cephalopod shells, rare tentaculites, and numerous conodonts (besides the index species of the *Pa. gigas* Z., i.e. *Pa. rhenana* age, numerous small elements of *Po.* cf. *webbi* have been regularly found in the rock - for reference sampling a well-accessible outcrop in the hillside between the Křtiny Marble Quarry and Křtiny-Babice-Josefov junction is recommended where the vegetation has been recently clear-cut). Some dark beds are interbedding the light limestone layers from the basinal side. This latest reef member (depth 162.3-214.2 m; Fig. 1) is similar to reef-cap or fore-reef bioherms of the Late Devonian sections of Roche Miette Mt. in Rocky Mountains of Alberta or Winterberg Hill in Harz Mountains of Germany. The both sites display similar composition of the rocks as well as evolution of the sequence in the terminating reef complex. This similarity reflect mostly the evolution in eustasy and global marine environment.

Fore-reef apron- to distal-slope sediments were drilled between 214.2 and 298.0 m (Fig. 1). This interval of depths is dominated by calciturbidites, having a bituminous clayey sedimentary background which was only sporadically influenced by slight contour resedimentation of winnowed sedimentary particles (low-energy environment). Rhythmic alternation of dark-grey detritic layers and blackish-grey shale by 3 to 5 cm prevails (cf. Dvořák et al. 1984). A decreased rate of cementation is indicated by slumping and convolute deformation structures. Bioturbation is poor or entirely absent. An overall absence of coral fauna is rarely interrupted by scattered coral or stromatoporoid heads (partly silicified pebbles; up to 20 cm in diameter; mostly *Actinostroma devonense*). These coral heads were mechanically abraded to a spherical shape and thrown down from the elevated reef margin. In distal forereef, they represent uncommon and exotic material.

Although some nodulated interbeds are scattered within the above mentioned fore-reef facies (in its uppermost and lowermost parts, especially), the underlying interval of the depths 298.0-329.0 m consists almost exclusively of nodular limestone. The reef-margin onland-climbing trajectory cut the vertical of the well immediately below this interval (cf. Fig. 1). High abundance of nodular limestones in neighbourhood of the reef margin assigns them to the proximal slope of the Frasnian reef complex whereas the calciturbidites of the overlying sequence belong to the distant part of the slope. The proximal part of the slope was sparsely grooved but not covered by the transported gravity-flow sediment. The lowermost part of this drilled interval displays numerous wash-out marks and coarse-grain intercalations. The pelagic-shell bioclastic spectrum was changed by rising number of crushed reefbuilders (reef apron).

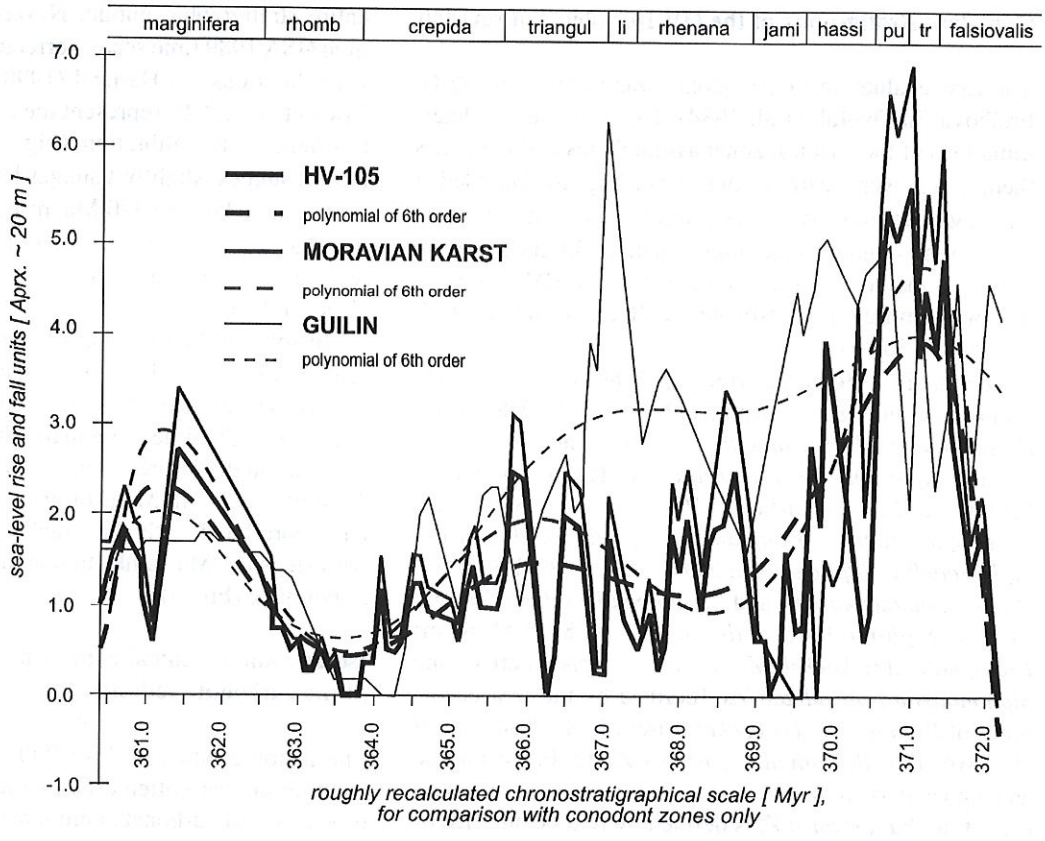


Fig. 4. The Frasnian-Famennian eustatic curves: an estimate for the HV-105 Křtiny borehole in comparison with average data for the Moravian Karst en masse (modified after Hladil 1988) and data from Guilin, China (after Shen 1995). Note the correspondence of many peaks as well as considerable similarity of the polynomial smoothed curves of the 6th order. Age on the horizontal axis (rising to right, Ma); sea-level fluctuation on the vertical axis (rising upwards, U ~ Aprx. 20 m)

Explanation of symbol ~ : relationship between the subjects, estimate

The underlying reef-margin sediments consist of diverse facies (329.0-369.0 m): stromatoporoid-coral framestone alternates with coral rubble, washed grainstone/rudstone of sand bars, bindstone with interlaced algal-coral coatings, mud-pool sediments, and rudstone/cement fills of reef caves. However, the reef margin was not steep or wall-shaped: the gently inclined reef margin (approximately 3 as documented on the geological section along the Křtiny Brook Valley; Hladil 1983) enabled an easy fluctuation of the reef margin forwards and backwards. The conodont record reaches as deep as the sediments of exposed reef-margin occur (334.0 m; Lower *Po. asymmetricus* Zone). Lack of conodonts is typical for the back reef facies in the lowermost third of the drilled section.

The core below 369.0 m shows exclusively the back-reef facies where typical *Amphipora*-limestone massively substituted the coral rubble and floatstone beds (cf. Fig. 1). Most of these Early Frasnian *Amphipora*-banks are storm-dependent event sequences which have similar stratification as carbonate mudbanks of present South-Florida. The sediment has dark colour; content of clay and quartz silt grains is negligible, dolomitisation is absent. The mudbank sedimentary environment is documented by weak abrasion of the *Amphipora*-stems together with the "in-situ breakdown" of the algal-stromatoporoid grass carpets (abundant *Issinella* segments of thalli).

We can summarise that the HV-105 reached the upper part of the Devonian carbonate complex of the Moravian Karst which was an integral part of the vast carbonate platforms on gently inclined southern-Laurussia continental margins. Dipping towards the axis of the Rhenish-type basins is assumed (transition reef/basin) and the late stage of the extension-transtension process is characterised by slow subsidence of the Brunovistulian crystalline basement.

General eustatic scenario: The tectonically caused fluctuation in the subsidence of this type had to bias the sedimentary record which was basically controlled by the global sea-level changes. These processes are indicated by differences form other reference curves (Fig. 4). Unfortunately, the Frasnian transtension (367 to 374 Ma) has never been modelled in detail. However, the general sea-level fluctuation pattern (Fig. 4) displays the same features as documented in the Australian Canning Basin or elsewhere in world: i.e., the transgressive onlap of the reef-margin facies was effective until the Middle Frasnian *Pa. punctata* times when an opposite downlap movement prevailed (cf. Dvořák et al. 1984). The Late Frasnian (*Pa. rhenana*) basinward retreating of the reef sediments is pronounced, almost reaching the sea level stands of the earliest Frasnian. A subsequent very strong Early Famennian lowstand was accompanied by the catastrophic impoverishment of the reef benthos as reflected also by an extreme narrowing of the coral-stromatoporoid carbonate platforms. These platforms were replaced by lime-mud ramps which were placed mostly on the frontal parts of the extinct coral banks whereas the back-end of the extinct banks was emerged.

## Conodont stratigraphy of the HV-105: object of revision

The first evaluation of conodonts was carried out by O. Friáková (in Dvořák et al. 1984). Of course, these determinations of the species, zonal assemblages and the zones themselves were carried out according to knowledge which was valid twelve years ago (cf. Figs. 1 and 3). Since the current standard conodont zonation differs from the previous, the conodont assemblages of the HV-105 borehole were entirely reinvestigated (collections of the Czech Geological Survey).

The main differences from the 1984 conodont determinations and zone stratigraphy are: 76.7-81.0 m: *Pseudopolygnathus triangulus triangulus* and lower part of the *Siphonodella crenulata* Zs. (O. Friáková) = *Siphonodella crenulata* Z. // 83.1-84.4 m: *Pseudopolygnathus triangulus inaequalis* Z. (O. Fr.) = *Siphonodella duplicata/sandbergi* Zs. // 87.0-88.0 m: *Protognathodus kockeli* and *Siphonodella sulcata* Zs. (O. Fr.) = *Siphonodella sulcata* Z. // 88.2-88.6 m: *Protognathodus kockeli* Z. (O. Fr.) = upper part of the *Siphonodella praesulcata* Zs. [defined by the first occurrence of *Protognathodus kockeli* Bischoff; 88.2-88.3 m]. // 89.0-108.0 m: *Bispathodus costatus* Z. (O. Fr.) = middle and upper part of the *Palmatolepis expansa* Z. [middle part of the *Pa. expansa* Z. is defined by first occurrence of *Bispathodus costatus* E. R. Branson and *Bi. aculeatus aculeatus* (Branson et Mehl); the lower part of the *Pa. expansa* and *Pa. postera* Zs. are missing or very reduced in thickness] // 110.0 m: *Polygnathus styriacus* Z. (O. Fr.) = *Pa. trachytera* Z. // 110.0-122.0 m: *Scaphignathus velifer* Z. (O. Fr.) = *Pa. trachytera* Z. [defined by occurrences of the conodont taxa *Pa. rugosa trachytera* Ziegler, *Pa. glabra lepta* Holmes, *Pa. minuta minuta* Branson et Mehl; together with *Po. perplexus* (Thomas)] // The determinations between the depths of 130 and 170 m are similar to the 1984 report, with an exception for the base of *Pa. rhenana* Z. [~ base of the *Pa. gigas* Z.] which is suggested to be deeper in the section, in the depth of 176.2 m // 176.2-198.6 m: ?*Ancyrognathus triangularis* Z. (O. Fr.) = the assemblage does not confirm this zone (this zone is missing or very reduced in the thickness) // beginning from the depth of 180.3 m and down to the last conodont evidences at 334 m, all assemblages belong to *Po. asymmetricus* Zs. [lower part of the *Pa. hassi*, *Pa. transitans* and *Me. falsiovalis* Zs. cannot be defined with great accuracy because of the dominance of *Icriodus* spp., *Ancyrodella rotundiloba rotundiloba*, *An. rotundiloba alata*, *Ozarkodina* spp., *Ligonodina* spp.]. The additional sedimentological and coral-stromatoporoid scaling had to be applied within the ranges of the *Po. asymmetricus* Zs.

## Numerical scaling of the time: a rough approximation to recent "best estimates"

The isotopic ages of the Late Devonian conodont zones are still insufficiently based, as generally accepted by the entire stratigraphic public. Nevertheless, the most common GSA 1989 time scale, corrected by the SDS conodont zone durations, cf. Harland (1990), Fordham (1992), and Crick et al. (1994), represent the current stage of the chronostratigraphic calibration (Fig. 3). Gradstein and Ogg (1996) suggest slightly younger bases of the Givetian and Frasnian, at 380 and 370 Ma, respectively, but this correction has been recently criticised for an incompatibility with the continuous logging of sedimentary sequences (Crick 1996).

In spite of the incorrectness of the absolute numerical scaling by age, this tool enables the time correlation among the lithological, isotope, eustatic and tectonic data. In addition, the time scale maintains the visualisation. For that, although we are aware of all constraints, the recent "best estimates" in Ma (Fordham 1992, Crick 1994) have been correlated with the graphic scale and recalculated with steps 0.1 Ma. Links to conodont zones have primary importance (Fig. 3).

## Isotope and chemical composition of the carbonate sediments

The isotopic ratios of $^{18}O/^{16}O$, $^{13}C/^{12}C$ and chemical analyses are very often used to trace processes involved in production of carbonate components and their subsequent conversion into limestones. Consequently, measured isotopic composition may reflect both the original deposition conditions or conditions during stabilisation of metastable carbonate phases.

Whole-rock chemical and isotopic data clearly reflect all phases of limestone formation; therefore if possible, it is better to separate fossils from their matrix, or separate individual generations of cements to obtain more information. Fossils represent a special case: the organic coating around their calcite crystals partly protects them from attack by solutions and they may preserve their original chemical and isotopic composition.

If the sediment is altered in low degree, the difference in isotopic composition of different components is preserved, being in relation to their type and origin. If the sediment is altered in high degree, the isotopic composition of the rock is mostly unified and it differs from the initial marine values.

Another possibility how to estimate the degree of alteration is a change in chemistry of carbonates. Brand - Veizer (1981) demonstrated that diagenetic stabilisation of carbonate components by meteoric waters was accompanied by decrease in $Sr^{2+}$ and $Na^{+}$. In consequence, this process is indicated by a distinct negative shift in $\delta^{18}O$ values and by an increase in $Mn^{2+}$ and $Fe^{2+}$ contents in diagenetically more stable low-Mg calcite. Especially, the decrease in amount of $Sr^{2+}$ together with increase in amount of $Mn^{2+}$ are good indicators of diagenetic alteration. The cements with low $\delta^{13}C$ values are formed when active pore water involves bicarbonate rich in $^{12}C$ (e.g. bi-

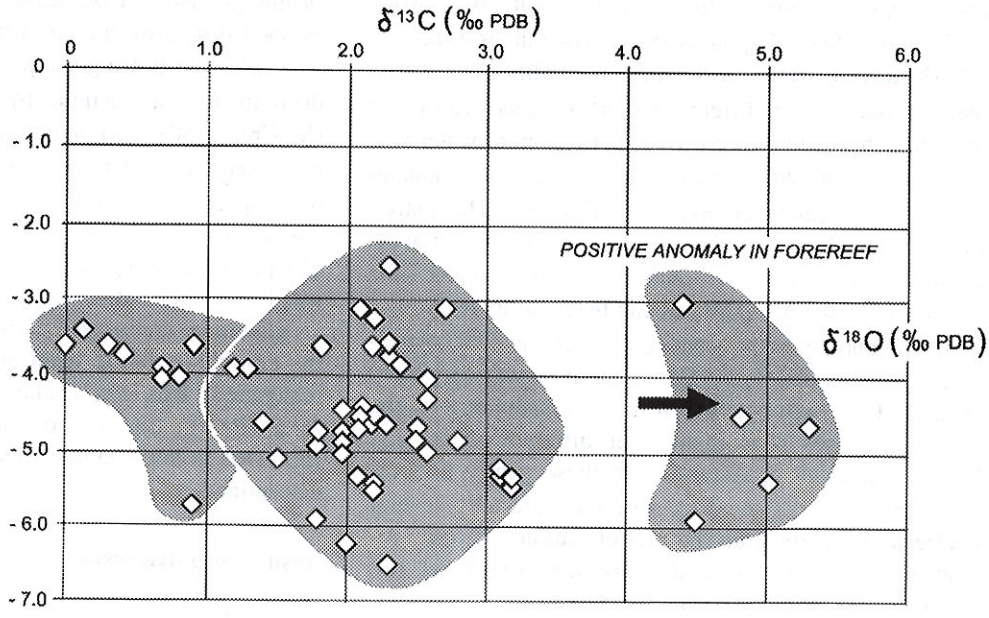


Fig. 5. C and O isotopes: relation between the $\delta^{13}C$ and $\delta^{18}O$ values. Due to diagenesis in closed pore-water/rock system, no visible diagenetical pathways are visible. The system shows an overall dispersal where the main differences consist in three $\delta^{13}C$ positions: about the values of 2.0 to 2.5 ~ bioherms, lagoons away of shore, some parts of forereef; about the values of 0.0 to 0.5 ~ backreef with algal grass; 4.5 to 5.5 ~ a facies-related anomaly which was developed in forereef during the maximum of transgression and opening of a local window for upwelling (below 371 Ma ~ standard conodont *transitans* Zone)

carbonate of biogenic origin). During the reaction of carbonate with pore water, the $\delta^{18}O$ values slowly decrease and the magnitude of this decrease depends on temperature and water/carbonate ratio, the decrease in $\delta^{18}O$ is accompanied by lowering in the $Sr^{2+}$ and $Mg^{2+}$ contents (Baker et al. 1982). Thus, joint interpretation of isotopic and chemical data can provide more information on the history of the carbonate rock.

## Carbon isotope excursions and global events

Analysis of global isotopic events indicates that the climatic control was significant (cf. Holser et al. 1995, Morrow et al. 1995, Walliser 1995). The dark-sediment events with an evident mass extinction of organisms reflected regularly extraordinary sea-level changes, i.e. the sea-level fall-and-rise couplet of extreme amplitudes, or the related cooling-warming fluctuations of high amplitudes, or the pulses in volcanic activity of inter-regional significance and extraordinary magnitude. The recent attempts to explain mechanism of crises related to dark-sediments seem to be divided into two groups: first operating with the multi-factor interacting systems where complementary starting agents of low order and random origination use to play the role of activators (Hladil - Kalvoda 1993), the second one operating with causal rows of distal-proximal effects (May 1995, Krhovský - Čejchan 1995). These causal rows use to be primarily developed from the climatic changes as recorded by the pronounced increase/decrease of polar ice caps with consequent fall/rise of sea level. The other concepts emphasise oscillating self-regulation of the biosphere-hydrosphere-atmosphere system. Most recent isotope studies are aimed at the causal explanation of global events.

Increased accumulation of organic carbon in the dark-event sediment corresponds to burial of organic matter under the condition of poor recycling back to the biosphere (Joachimski - Buggisch 1992, 1993). Periods of increased accumulation of organic carbon are characterised by higher contents of $^{13}C$ in carbonates. McGhee et al. (1986) found the Late Devonian Kellwasser dark sequences independent on possible abrupt cessation of the phytoplankton activity because no sharp drops in the $\delta^{13}C$ values were indicated in the section of Steinbruch Schmidt. Joachimski - Buggisch (1992) stated that the strangelove effect of mass biota killing and impoverishment was absent and the positive shifts in C-isotope composition appeared not only during advanced crises but as well during the post crisis recovery. Increased primary productivity was typical for the crises and subsequent stages of the biotic recoveries.

Three major positive $^{13}C$-anomalies have been recognised in the Middle to Upper Devonian carbonates: (I) the Late Givetian anomaly, Wolayer Gletscher, Austrian Alps; (II) the Lower Kellwasser anomaly, in Early *rhenana* Zone, and (III) the anomaly beginning at the Frasnian/Famennian boundary, in *Pa. linguiformis* to *Pa. triangularis* Zone, Steinbruch Benner, Rhenish Slate Mts. (Joachimski - Buggisch 1992). The ultimate test for the real global nature of an isotopic event is its verification in distinct and distant sedimentary basins (Holser et al. 1995). In addition, the positive excursion of the $\delta^{13}C$ values must be found in different facies, i.e., in dark and light limestone beds. According to this test, the original assumption by Joachimski and Buggish about the global significance of these events has been more and more verified.

Although there is no doubt that composition of ocean water is controlled by global changes, the influence of sedimentary and diagenetical facies could not be omitted. In addition, the epicontinental basins yield commonly different conditions than the global ocean reservoir.

As a rule, the Rhenish fore-reef slope of the Devonian

reef complexes show regularly increased amounts of the $^{13}C$ isotope (Jux - Zygojanis 1983). The ranges of this facial fluctuation were documented in conditions of recent reef complexes: The difference in $\delta^{13}C$ values can reach up to 8 ‰ between the zone of upper-reef pore-water/sea-water wind-derived pressure and proximal carbonate-complex slope can reach up to 8 ‰ (Sansone - Haberstroh 1995), although part of this difference can be a result of diagenesis. According to Sansone and Haberstroh (1995) the differences in the $\delta^{18}O$ values can reach up to 10 ‰.

In comparison with recent conditions, the $\delta^{13}C$ facies-related gradient of the Late Devonian times was very steep because of the high position of the dark sediments on the carbonate slopes (documented in different areas, e.g. Alberta, Moravia, or Asturia). On these gently inclined slopes (about 2-3°), the dark sediments are only several hundreds of meters from the reef elevation, i.e., only several tens metres below the Frasnian sea level (cf. Hedinger - Workum 1988, Geldsetzer 1988).

Owing to patchy pattern of disoxy in epicontinental seas, we assume strong local fluctuations in isotope composition of the Late Devonian carbonate rocks. In our opinion, the current stage of the documentation meets essentially two problems: discrimination of the local and global influences and lack of documentation among the prominent "crisis or boundary levels" which were main subject of the previous studies. It is possible, that significant isotope anomalies are still unknown because the both vertical and horizontal sectioning of the Late Devonian carbonate complexes is very fragmentary. These missing anomalies could have the global or local significance. Theoretically, the local anomalies must correspond to the regional windows in the stratification of the ocean water or patchy pattern in sedimentology and diagenesis (cf. the model of regionally bounded disturbances in the stratified ocean, Wilde et al. 1990). Of course, the global and local changes are not strongly separated; feedback or accelerating processes are known, e.g. El Nino effect or area of submerged shelfs.

Brief logging of C and O isotope data from the Moravian Karst reef margin based on the Křtiny HV-105 core drilling aims to contribute the existing data background for the Devonian interval between the Pre-*asymmetricus* and Kellwasser events. There is also a strong implication for possible facial dependence of the $\delta^{13}C$ anomalies.

## Material and methods

The samples were taken from fifteen different depths of the drilled core (Fig. 1). These samples represent the main facies types of the section. Different carbonate phases were drilled out by dentist drilling machine from polished section and used for isotopic and chemical analyses. The sample collection from HV-105 (Tab. 1, Fig. 2) involved a variety of fossils (corals, stromatoporoids), various types of fine grained matrix, and the later components (cements in open structures, fracture fills).

Carbonate-bearing samples for isotopic analyses were decomposed in vacuum by 100% $H_3PO_4$ at 25 °C (McCrea 1950). Carbon and oxygen isotopic composition of released $CO_2$ was measured on a Finnigan MAT 251 mass spectrometer. The results are reported in per mille deviations from the PDB standard using the $\delta$ notation. The precision of both carbon and oxygen isotope analyses was better than ± 0.1 ‰.

Chemical analyses: Calcium content was determined by complexometric titration; magnesium, strontium, manganese, iron ($Fe_{tot}$) and sodium were determined by AAS (Perkin Elmer 3100) after decomposition in hot HCl. Due to low quantity of sample total carbon was not determined.

## Results and discussion

The results of the isotopic and chemical analyses have been summarised in a spreadsheet, including the simplified description, sample depth and numbers (Tab. 1). The $\delta^{13}C$ values range from 0.0 to 5.3 ‰, the $\delta^{18}O$ values range from -6.5 to -2.5 ‰ PDB. The content of calcium in samples fluctuates between 37.8 and 40.4 %; such very high Ca-content confirms the pureness of carbonate rocks. The content of Mg varies from 0.2 to 0.4 %, the content of Mn ranges from 40 to 180 ppm (only one sample contains 760 ppm), content of total Fe ($Fe_{tot}$) is in hundreds of ppm (rarely, is higher than 1000 ppm), the ratio 1000 Sr/Ca varies between 0.35 a 0.86. Individual components of the rock were analysed separately: e.g. the tabulate corals, rugose corals, amphiporids, stachyodids, massive stromatoporoids, various types of the matrix and cement, fills of open structures, stromatactis or fracture fills and veins (cf. Tab. 1, Fig. 7).

## Fossils

Preservation of the primary isotope and chemical composition of carbonate fossils depends on preservation of primary/early mineralogy of the skeletons (Hudson 1977). The tabulate corals consisted of low- to intermediate-Mg-calcite, the rugose corals of high-Mg-calcite and the demospongian stromatoporoids used mostly high-Mg-calcite and aragonite for building of their coenostea (Zorn 1977, Mistiaen 1984, Brand - Veizer 1981) and it is known that the latter two phases belong to less stable carbonate components. In samples from the HV-105, the all skeletons consist of calcite which has very low content of Mg (LMC). For that reason, they cannot reflect directly the sedimentary conditions but they document the superimposed diagenetical equalisation/compensation of the values, i.e. the stage when the metastable carbonate structure was changed to the more stable calcite.

**Rugose corals:** As recognised by Milliman (1974) and

Table 1. Samples: spreadsheet of the isotope and chemical analyses from the HV-105 Křtiny borehole. The text data about the nature of the analysed rock components are included (left)

| sample No | description of samples | rock component | stage / part | conodont zone | depth (m) | age Aprx. (Myr) | $\delta^{13}C$ (‰ PDB) | $\delta^{18}O$ (‰ PDB) | Ca (%) | Mg (%) | Sr (ppm) | Mn (ppm) | Fe (ppm) | Na (ppm) | 1000 Sr/Ca | 1000 Mg/Ca |
|---|---|---|---|---|---|---|---|---|---|---|---|---|---|---|---|---|
| 2050 | 1-1 stromatactis structure | cement | L. Famennian | Pa. marginifera | 124.5 | 360.2 | 2.2 | -3.6 | 39.98 | 0.20 | 160 | 147 | 510 | 148 | 0.40 | 4.95 |
| 2051 | 1-2 lime-mudstone matrix | matrix | L. Famennian | Pa. marginifera | 124.5 | 360.2 | 1.3 | -3.9 | 39.69 | 0.32 | 190 | 179 | 1190 | 74 | 0.48 | 8.01 |
| 2052 | 1-3 nodule of laminated wackestone | matrix | L. Famennian | Pa. marginifera | 124.5 | 360.2 | 0.7 | -3.9 | 37.81 | 0.31 | 200 | 150 | 910 | 74 | 0.53 | 8.09 |
| 2053 | 1-4 nodule of intraclastic packstone | matrix | L. Famennian | Pa. marginifera | 124.5 | 360.2 | 1.2 | -3.9 | | | | | | | | |
| 2054 | 2-1 wackestone in a nodule | matrix | L. Famennian | Pa. marginifera | 140.0 | 362.0 | 2.1 | -3.1 | | | | | | | | |
| 2055 | 2-2 lime-mudstone matrix | matrix | L. Famennian | Pa. marginifera | 140.0 | 362.0 | 0.9 | -5.7 | | | | | | | | |
| 2056 | 2-3 calcite veins | cement | L. Famennian | Pa. marginifera | 140.0 | 362.0 | 1.8 | -4.7 | | | | | | | | |
| 2057 | 3-1 Actinostroma sp. | stromatoporoid | L. Frasnian | Pa. rhenana | 166.7 | 368.0 | 2.3 | -2.5 | 40.45 | 0.21 | 150 | 74 | 190 | 53 | 0.37 | 5.16 |
| 2058 | 3-2 Stachyodes lagowiensis | stachyodid | L. Frasnian | Pa. rhenana | 166.7 | 368.0 | 2.3 | -4.6 | 39.95 | 0.20 | 150 | 63 | 380 | 134 | 0.37 | 5.01 |
| 2059 | 3-3 Scoliopora denticulata | tabulate coral | L. Frasnian | Pa. rhenana | 166.7 | 368.0 | 2.3 | -6.5 | 40.35 | 0.23 | 150 | 77 | 590 | 74 | 0.37 | 5.58 |
| 2060 | 3-4 matrix with stachyodid debris | matrix | L. Frasnian | Pa. rhenana | 166.7 | 368.0 | 2.2 | -4.6 | 39.19 | 0.24 | 180 | 70 | 530 | 104 | 0.46 | 6.12 |
| 2061 | 3-5 matrix with intraclastic debris | matrix | L. Frasnian | Pa. rhenana | 166.7 | 368.0 | 2.0 | -6.2 | 39.64 | 0.28 | 160 | 113 | 1470 | 57 | 0.41 | 7.11 |
| 2062 | 3-6 matrix with debris of algae, molluscs | matrix | L. Frasnian | Pa. rhenana | 166.7 | 368.0 | 2.3 | -3.7 | 39.62 | 0.24 | 150 | 67 | 350 | 28 | 0.38 | 6.06 |
| 2063 | 3-7 micrite of clastic origin | matrix | L. Frasnian | Pa. rhenana | 166.7 | 368.0 | 2.2 | -3.2 | 39.87 | 0.23 | 180 | 57 | 200 | 134 | 0.45 | 5.87 |
| 2068 | 5-1 Alveolites complanatus | tabulate coral | L. Frasnian | Pa. rhenana | 178.4 | 368.8 | 2.4 | -3.8 | 40.05 | 0.34 | 250 | 81 | 220 | 104 | 0.62 | 8.39 |
| 2069 | 5-2 Actinostroma sp. | stromatoporoid | L. Frasnian | Pa. rhenana | 178.4 | 368.8 | 1.8 | -4.9 | 40.05 | 0.34 | 240 | 759 | 700 | 74 | 0.58 | 8.18 |
| 2070 | 5-3 Scoliopora kaisini | tabulate coral | L. Frasnian | Pa. rhenana | 178.4 | 368.8 | 2.6 | -4.3 | 40.44 | 0.34 | 320 | 81 | 460 | 58 | 0.79 | 8.46 |
| 2071 | 5-4 Stachyodes regularis | stachyodid | L. Frasnian | Pa. rhenana | 178.4 | 368.8 | 2.3 | -3.5 | 40.61 | 0.41 | 340 | 71 | 210 | 126 | 0.82 | 9.95 |
| 2072 | 5-5 algal crusts | alga | L. Frasnian | Pa. rhenana | 178.4 | 368.8 | 2.5 | -4.8 | 39.96 | 0.30 | 310 | 110 | 330 | 378 | 0.78 | 7.51 |
| 2073 | 5-6 grainstone matrix | matrix | L. Frasnian | Pa. rhenana | 178.4 | 368.8 | 2.6 | -5.0 | 39.59 | 0.29 | 290 | 82 | 430 | 82 | 0.73 | 7.27 |
| 2074 | 5-7 rugose coral | rugose coral | L. Frasnian | Pa. rhenana | 178.4 | 368.8 | 2.7 | -3.1 | 39.98 | 0.21 | 140 | 91 | 150 | 104 | 0.35 | 5.25 |
| 2064 | 4-1 abradded coenosteum, Actinostroma sp. | stromatoporoid | M. Frasnian | ?Pa. hassi | 220.0 | 370.6 | 1.8 | -3.6 | | | | | | | | |
| 2065 | 4-2 crinoidal packstone | matrix | M. Frasnian | ?Pa. hassi | 220.0 | 370.6 | 2.0 | -4.9 | | | | | | | | |
| 2066 | 4-3 intra/extraclastic packstone | matrix | M. Frasnian | ?Pa. hassi | 220.0 | 370.6 | 2.1 | -4.4 | | | | | | | | |
| 2067 | 4-4 lime-mudstone | matrix | M. Frasnian | ?Pa. hassi | 220.0 | 370.6 | 1.5 | -5.1 | | | | | | | | |
| 2079 | 7-1 Actinostroma tabulatum | stromatoporoid | E. Frasnian | ?Pa. transitans | 252.0 | 371.0 | 4.8 | -4.5 | 40.42 | 0.19 | 220 | 25 | 70 | 53 | 0.53 | 4.49 |
| 2075 | 6-1 Actinostroma tabulatum | stromatoporoid | E. Frasnian | ?Pa. transitans | 276.0 | 371.3 | 4.4 | -3.0 | 39.75 | 0.28 | 220 | 49 | 60 | 89 | 0.55 | 7.09 |
| 2076 | 6-2 Temnophyllum sp. | rugose coral | E. Frasnian | ?Pa. transitans | 276.0 | 371.3 | 4.5 | -5.9 | 40.09 | 0.28 | 340 | 39 | 70 | 51 | 0.85 | 6.88 |
| 2077 | 6-3 extraclastic/bioclastic packstone | matrix | E. Frasnian | ?Pa. transitans | 276.0 | 371.3 | 5.0 | -5.4 | 39.49 | 0.39 | 340 | 50 | 110 | 193 | 0.86 | 9.87 |
| 2078 | 6-4 calcisiltite nodules | matrix | E. Frasnian | ?Pa. transitans | 276.0 | 371.3 | 5.3 | -4.6 | | | | | | | | |
| 2080 | 8-1 Alveolites delhayei | tabulate coral | E. Frasnian | ?Me. falsiovalis | 334.8 | 372.2 | 2.2 | -4.5 | 39.32 | 0.26 | 220 | 96 | 240 | 53 | 0.56 | 6.56 |
| 2081 | 8-2 Hermatostroma sp. | stromatoporoid | E. Frasnian | ?Me. falsiovalis | 334.8 | 372.2 | 2.0 | -4.4 | 40.23 | 0.31 | 240 | 71 | 170 | 72 | 0.58 | 7.57 |
| 2082 | 8-3 packstone nodule | matrix | E. Frasnian | ?Me. falsiovalis | 334.8 | 372.2 | 2.1 | -5.3 | | | | | | | | |
| 2083 | 8-4 grainstone matrix | matrix | E. Frasnian | ?Me. falsiovalis | 334.8 | 372.2 | 1.8 | -5.9 | 39.59 | 0.29 | 230 | 113 | 470 | 65 | 0.58 | 7.43 |
| 2084 | 8-5 Thamophyllum monozonatum | rugose coral | E. Frasnian | ?Me. falsiovalis | 334.8 | 372.2 | 2.1 | -4.6 | 40.10 | 0.25 | 200 | 50 | 70 | 48 | 0.50 | 6.13 |
| 2085 | 9-1 Clathrocoilona sp. | stromatoporoid | E. Frasnian | ?Me. falsiovalis | 342.3 | 372.3 | 1.4 | -4.6 | | | | | | | | |
| 2086 | 9-2 Thamnopora boloniensis | tabulate coral | E. Frasnian | ?Me. falsiovalis | 342.3 | 372.3 | 2.0 | -4.7 | 40.23 | 0.34 | 160 | 133 | 120 | 119 | 0.39 | 8.15 |
| 2087 | 9-3 Hermatostroma sp. | stromatoporoid | E. Frasnian | ?Me. falsiovalis | 342.3 | 372.3 | 2.1 | -4.5 | | | | | | | | |
| 2088 | 9-4 Amphipora laxeperforata | amphiporid | E. Frasnian | ?Me. falsiovalis | 342.3 | 372.3 | 2.2 | -5.4 | 40.60 | 0.31 | 330 | 159 | 390 | 556 | 0.76 | 7.02 |
| 2089 | 9-5 packstone/grainstone | matrix | E. Frasnian | ?Me. falsiovalis | 342.3 | 372.3 | 2.0 | -5.0 | 39.71 | 0.31 | 290 | 124 | 320 | 97 | 0.73 | 7.86 |
| 2090 | 10-1 Disphyllum regulare | rugose coral | E. Frasnian | ?Me. falsiovalis | 379.7 | 372.5 | 2.8 | -4.8 | 39.66 | 0.23 | 180 | 40 | 80 | 22 | 0.45 | 5.75 |
| 2091 | 10-2 Alveolites mailleuxi | tabulate coral | E. Frasnian | ?Me. falsiovalis | 379.7 | 372.5 | 3.2 | -5.4 | | | | | | | | |
| 2092 | 10-3 biocementstone, massive | matrix | E. Frasnian | ?Me. falsiovalis | 379.7 | 372.5 | 3.1 | -5.2 | | | | | | | | |
| 2093 | 10-4 carbonate veins in fractured rocks | cement | E. Frasnian | ?Me. falsiovalis | 379.7 | 372.5 | 2.6 | -4.0 | | | | | | | | |
| 2094 | 11-1 Amphipora rudis | amphiporid | E. Frasnian | ?Me. falsiovalis | 413.0 | 372.8 | 3.2 | -5.3 | | | | | | | | |
| 2095 | 11-2 packstone with green-alga tubes | matrix | E. Frasnian | ?Me. falsiovalis | 413.0 | 372.8 | 3.1 | -5.3 | | | | | | | | |
| 2096 | 12-1 Amphipora pinguis | amphiporid | E. Frasnian | ?Me. falsiovalis | 434.4 | 372.9 | 2.5 | -4.6 | | | | | | | | |
| 2097 | 12-2 biointraclastic packstone | matrix | E. Frasnian | ?Me. falsiovalis | 434.4 | 372.9 | 2.2 | -5.5 | | | | | | | | |
| 2098 | 13-1 Amphipora angusta | amphiporid | ?L. Givetian | ?Kl. disparilis | 461.4 | 373.2 | 0.8 | -4.0 | | | | | | | | |
| 2099 | 13-2 packstone with Amphipora debris | matrix | ?L. Givetian | ?Kl. disparilis | 461.4 | 373.2 | 0.7 | -4.0 | | | | | | | | |
| 2100 | 13-3 plasticlast of poorly washed grainstone | lithoclast | ?L. Givetian | ?Kl. disparilis | 461.4 | 373.2 | 0.9 | -3.6 | | | | | | | | |
| 2101 | 14-1 Amphipora angusta | amphiporid | ?L. Givetian | ?Kl. disparilis | 494.5 | 373.2 | 0.4 | -3.7 | | | | | | | | |
| 2102 | 14-2 recrystallized micrite with algae | matrix | ?L. Givetian | ?Kl. disparilis | 494.5 | 373.6 | 0.3 | -3.6 | | | | | | | | |
| 2103 | 15-1 Amphipora angusta | amphiporid | ?L. Givetian | ?Kl. disparilis | 502.3 | 373.6 | 0.0 | -3.6 | 40.19 | 0.29 | 320 | 74 | 40 | 52 | 0.79 | 7.32 |
| 2104 | 15-2 Amphipora/brachiopod packstone | matrix | ?L. Givetian | ?Kl. disparilis | 502.3 | 373.6 | 0.1 | -3.4 | 40.41 | 0.29 | 260 | 54 | 170 | 178 | 0.61 | 6.71 |

Table 2. Sea-level fluctuation: spreadsheet of the data calculated for the sea-level changes in the HV-105 borehole, Moravian Karst block en masse and a distant region of Guilin in China (a biofacially derived eustatic curve, Shen 1995). For comparison with Figs. 3 and 4, 6 and 7

| 1 | sea-level rise and fall (recalc.) | | | 2 (cont.) | sea-level rise and fall (recalc.) | | | 3 (cont.) | sea-level rise and fall (recalc.) | | |
|---|---|---|---|---|---|---|---|---|---|---|---|
| Aprx. time level | HV-105 borehole | GUILIN China - after Shen | MORAV. KARST en masse | Aprx. time level | HV-105 borehole | GUILIN China - after Shen | MORAV. KARST en masse | Aprx. time level | HV-105 borehole | GUILIN China - after Shen | MORAV. KARST en masse |
| 360.4 | 1.4 | 1.6 | 1.7 | 364.4 | 0.6 | 0.5 | 0.8 | 368.4 | 1.8 | 2.5 | 2.2 |
| 360.5 | 1.4 | 1.6 | 1.7 | 364.5 | 1.3 | 1.3 | 1.5 | 368.5 | 1.9 | 2.3 | 2.8 |
| 360.6 | 1.6 | 1.6 | 2.0 | 364.6 | 1.3 | 2.0 | 1.5 | 368.6 | 1.9 | 2.1 | 3.4 |
| 360.7 | 1.9 | 1.6 | 2.3 | 364.7 | 1.0 | 2.2 | 1.2 | 368.7 | 2.5 | 1.9 | 3.1 |
| 360.8 | 1.6 | 1.6 | 2.0 | 364.8 | 1.0 | 1.9 | 1.2 | 368.8 | 1.9 | 1.7 | 2.3 |
| 360.9 | 1.5 | 1.6 | 1.9 | 364.9 | 0.9 | 1.6 | 1.1 | 368.9 | 1.5 | 1.6 | 1.9 |
| 361.0 | 1.0 | 1.7 | 1.2 | 365.0 | 0.9 | 1.3 | 1.1 | 369.0 | 0.6 | 2.1 | 0.8 |
| 361.1 | 0.6 | 1.7 | 0.8 | 365.1 | 0.6 | 1.0 | 0.8 | 369.1 | 0.6 | 2.6 | 0.6 |
| 361.2 | 1.5 | 1.7 | 1.9 | 365.2 | 1.3 | 1.3 | 1.5 | 369.2 | 0.0 | 3.1 | 0.5 |
| 361.3 | 2.1 | 1.7 | 2.6 | 365.3 | 1.5 | 1.7 | 1.9 | 369.3 | 0.4 | 3.6 | 0.3 |
| 361.4 | 2.8 | 1.7 | 3.4 | 365.4 | 1.0 | 2.2 | 1.2 | 369.4 | 1.8 | 4.1 | 0.2 |
| 361.5 | 2.6 | 1.7 | 3.2 | 365.5 | 1.0 | 2.3 | 1.2 | 369.5 | 0.8 | 4.5 | 0.0 |
| 361.6 | 2.5 | 1.7 | 3.1 | 365.6 | 1.0 | 2.3 | 1.2 | 369.6 | 0.8 | 4.0 | 0.0 |
| 361.7 | 2.4 | 1.8 | 2.9 | 365.7 | 1.3 | 1.8 | 1.5 | 369.7 | 2.8 | 4.4 | 1.5 |
| 361.8 | 2.3 | 1.8 | 2.8 | 365.8 | 2.5 | 1.4 | 3.1 | 369.8 | 1.9 | 5.0 | 0.0 |
| 361.9 | 2.1 | 1.8 | 2.6 | 365.9 | 2.5 | 1.0 | 3.0 | 369.9 | 4.0 | 5.1 | 1.5 |
| 362.0 | 2.0 | 1.7 | 2.5 | 366.0 | 1.9 | 1.4 | 2.3 | 370.0 | 3.1 | 4.9 | 1.2 |
| 362.1 | 1.9 | 1.7 | 2.3 | 366.1 | 1.3 | 1.8 | 1.5 | 370.1 | 2.5 | 4.7 | 1.5 |
| 362.2 | 1.8 | 1.7 | 2.2 | 366.2 | 0.6 | 2.1 | 0.8 | 370.2 | 1.9 | 4.5 | 2.3 |
| 362.3 | 1.6 | 1.6 | 2.0 | 366.3 | 0.0 | 2.3 | 0.0 | 370.3 | 1.3 | 4.3 | 4.3 |
| 362.4 | 1.5 | 1.6 | 1.9 | 366.4 | 0.6 | 2.5 | 0.8 | 370.4 | 0.6 | 4.7 | 2.0 |
| 362.5 | 1.4 | 1.6 | 1.7 | 366.5 | 2.0 | 2.7 | 2.5 | 370.5 | 1.0 | 4.8 | 3.1 |
| 362.6 | 1.3 | 1.5 | 1.5 | 366.6 | 1.9 | 2.0 | 2.4 | 370.6 | 4.5 | 4.9 | 5.6 |
| 362.7 | 0.8 | 1.4 | 0.9 | 366.7 | 1.9 | 2.2 | 2.3 | 370.7 | 5.4 | 5.0 | 6.6 |
| 362.8 | 0.8 | 1.4 | 0.9 | 366.8 | 1.3 | 3.9 | 1.5 | 370.8 | 5.0 | 4.0 | 6.2 |
| 362.9 | 0.5 | 1.3 | 0.6 | 366.9 | 0.3 | 3.6 | 0.3 | 370.9 | 5.4 | 3.1 | 6.6 |
| 363.0 | 0.6 | 1.1 | 0.8 | 367.0 | 0.3 | 6.3 | 0.3 | 371.0 | 5.6 | 2.1 | 7.0 |
| 363.1 | 0.3 | 0.9 | 0.3 | 367.1 | 1.8 | 5.7 | 2.2 | 371.1 | 3.8 | 4.6 | 4.6 |
| 363.2 | 0.3 | 0.7 | 0.4 | 367.2 | 1.3 | 5.0 | 1.5 | 371.2 | 4.5 | 3.4 | 5.6 |
| 363.3 | 0.5 | 0.5 | 0.6 | 367.3 | 0.9 | 4.2 | 1.1 | 371.3 | 3.9 | 2.3 | 4.8 |
| 363.4 | 0.3 | 0.3 | 0.3 | 367.4 | 0.7 | 3.5 | 0.9 | 371.4 | 4.9 | 2.7 | 6.0 |
| 363.5 | 0.4 | 0.2 | 0.5 | 367.5 | 0.5 | 2.8 | 0.6 | 371.5 | 3.3 | 3.4 | 4.0 |
| 363.6 | 0.0 | 0.2 | 0.0 | 367.6 | 1.0 | 3.1 | 1.2 | 371.6 | 2.6 | 4.6 | 3.2 |
| 363.7 | 0.0 | 0.2 | 0.0 | 367.7 | 0.3 | 3.5 | 0.3 | 371.7 | 2.0 | 3.4 | 2.5 |
| 363.8 | 0.0 | 0.2 | 0.0 | 367.8 | 0.6 | 3.7 | 0.8 | 371.8 | 1.4 | 2.2 | 1.7 |
| 363.9 | 0.4 | 0.2 | 0.5 | 367.9 | 1.9 | 3.5 | 2.3 | 371.9 | 1.8 | 3.4 | 2.2 |
| 364.0 | 0.4 | 0.1 | 0.5 | 368.0 | 1.4 | 3.3 | 1.7 | 372.0 | 1.3 | 4.6 | 1.5 |
| 364.1 | 1.2 | 0.0 | 1.5 | 368.1 | 2.0 | 3.1 | 2.5 | 372.1 | 0.6 | 4.4 | 0.8 |
| 364.2 | 0.5 | 0.0 | 0.6 | 368.2 | 1.5 | 2.9 | 1.9 | 372.2 | 0.0 | 4.2 | 0.0 |
| 364.3 | 0.5 | 0.0 | 0.6 | 368.3 | 1.0 | 2.7 | 1.2 | | | | |

Brand (1981), the rugose corals secreted intermediate-Mg-calcite skeletons. Similarly to recent scleractinians, the rugose corals also incorporated metabolic oxygen into skeletal calcite and their corallum was not built in isotopic equilibrium with the marine water. Brand (1981) analysed the rugose corals and brachiopods of the Lower Pennsylvanian Kedric fauna (Eastern Kentucky). It is known that brachiopods secret calcite shells in isotopic equilibrium with sea water. The $\delta^{13}C$ values of the Kedric brachiopods were close to 1.7 ‰ , their $\delta^{18}O$ values were close to -5 ‰. The $\delta^{13}C$ values of the Kedric rugose corals were between -2.1 and 1.4 ‰, i.e. very close to the $\delta^{13}C$ values of the brachiopod shells, whereas $\delta^{18}O$ values of Kedric rugose corals were between -9.0 and -9.8 ‰. This low difference between the $^{13}C$-contents in brachiopods and rugose corals indicates that biological fractionation of carbon isotopes between Kedric rugose corals and Late Carboniferous sea-water had to be significantly lower than the fractionation of the oxygen isotopes. This pattern of fractionation is assumed for all Late Palaeozoic rugose corals, although a certain bias due to kinetic isotope effects in biological carbonates or early diagenetic specifics of rugosan HMC must be considered (cf. McConnaughey 1989).

The rugose corals from the HV-105 have the $\delta^{13}C$ values between 2.1 and 4.5 ‰ (in average 3.0 ‰). Their $\delta^{18}O$ values range between -5.9 and -3.1 ‰ (in average -4.6 ‰ PDB), cf. Tab. 1 and Fig. 7. It follows that $\delta^{13}C$ and $\delta^{18}O$ values of rugose corals from HV-105 are significantly higher than values reported by Brand (1981) for the American Late Carboniferous.

**Tabulate corals:** Carbon and oxygen isotope compositions of tabulate corals and stromatoporoids were documented by Jux - Manze (1976) on the material from the

Middle Devonian reefs in Bergischen Landes (Rhenish Slate Mts.). The mean values $\delta^{13}C$ and $\delta^{18}O$, -1.99 ‰ and -8.1 ‰, respectively, were found for the analysed favositids.

The $\delta^{13}C$ values of the tabulate corals from the HV-105 range from 2.0 to 3.2 ‰ (in average 2.45 ‰); the $\delta^{18}O$ values are between -3.8 and -6.5 ‰ PDB (in average -4.87 ‰), cf. Tab. 1, Fig. 7. It is clear that also $\delta^{13}C$ and $\delta^{18}O$ values for tabulate corals from HV-105 are significantly higher in comparison with the data reported by Jux - Manze (1976).

**Stromatoporoids:** Analysis of stromatoporoids is usually accompanied by bias in sampling because the very fine, recrystallised vesiculous microstructure can be hardly separated from the cement fills. The microdrilling of our stromatoporoid samples provided the material where also 40-60 % of later cement biased the results. For that reason the analyses of stromatoporoids have given information rather on composition of the early cement fills than on the soft, primary aragonite skeleton. Jux - Manze (1976) introduced for the stromatoporoids the following average values: $\delta^{13}C$: -1.66 ‰, and $\delta^{18}O$: -6.83 ‰ PDB.

The stromatoporoids analysed from the HV-105 showed the $\delta^{13}C$ values from 0.0 to 4.8 ‰ (in average 2.2 ‰) and $\delta^{18}O$ values from -5.4 to -2.5 ‰ PDB (in average -4.2 ‰).

Delicate branches of amphiporids have independent position among the analysed stromatoporoids. They were concentrated in back-reef position and their soft skeleton was formerly, in a very early stage of the diagenesis, replaced by fibre-radial clusters of high-Mg calcite. Our amphiporid samples from the HV-105 provided the $\delta^{18}O$ values from -6.5 to -2.5 ‰. The highest values found in these amphiporids are very similar to Late Devonian sedimentary values; they correspond to carbonate precipitated in equilibrium with Late Devonian sea water.

The $\delta^{13}C$ and $\delta^{18}O$ values of unaltered brachiopod shells are the best tool for estimation of isotopic composition in ancient sea water. Carpenter et al. (1991) found for the Late Devonian brachiopods the $\delta^{18}O$ values ranging from -3.5 to -6.5 ‰ and Brand (1989), who traced these isotopic compositions from North America to Eurasia, found for the brachiopods the $\delta^{18}O$ values between -9.7 and -3.6 ‰. The Late Devonian marine cements from the Golden Spike and Nevis Reefs in Alberta, Canada, show similar $\delta^{18}O$ values (Carpenter, Lohmann 1989). Unfortunately, separation of the brachiopods from the investigated slabs in the HV-105 failed due to their scarcity and compactness of the rocks.

## Matrix and cement

The type of matrix sampled from slabs of the HV-105 core differs in grain size; they vary from lime-mudstone to fine grained grainstone. This very fine mixture of clasts, cement and residue on solution sutures was technologically below the selectivity of the dentist drilling machine. The $\delta^{13}C$ values of matrix range from 0.1 to 5.3 ‰ (in average 2.14 ‰); the $\delta^{18}O$ values are between -6.2 and -3.2 ‰ (in average -4.43 ‰ PDB). The diagenetical alteration was mostly controlled by migration of fluids and this migration was enabled by the presence of pores in rock structure. For that reason, the micrite types of matrix which are characterised by low permeability are altered in lesser degree than the coarse and more porous types of rock matrix. In this way we can explain fairly different isotopic results for different types of matrix drilled from the same slab (Tab. 1, Fig. 6). It can be exemplified by the slab from the borehole depth 166.7 m where sample no. 2063 (micrite) has the $\delta^{18}O$ value of -3.2 ‰ but sample no. 2061 (matrix with intraclastic debris) showed the O

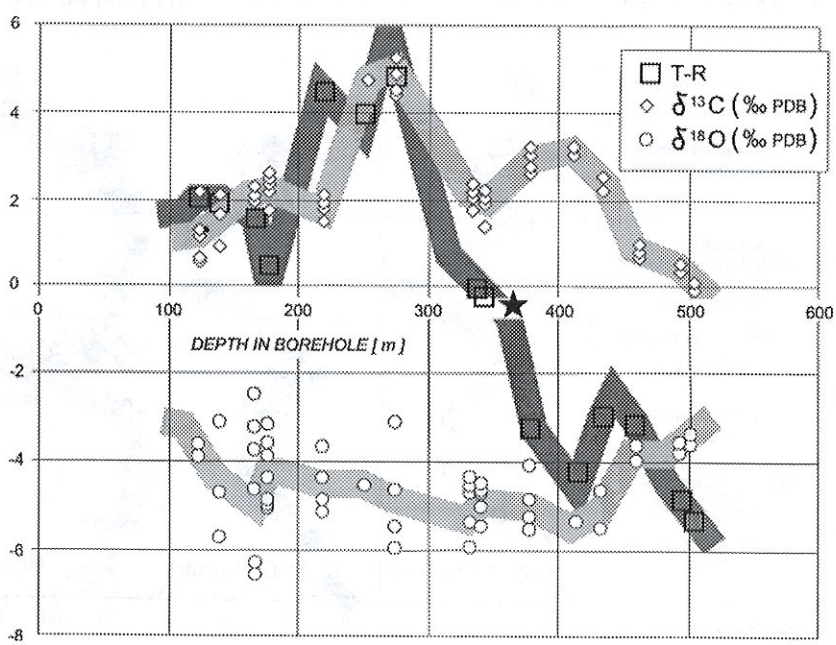


Fig. 6. C and O isotopes: comparison of the $\delta^{13}C$ and $\delta^{18}O$ values (‰ PDB) with the eustatic curve along the drilled section of the HV-105. Depth in meters on the horizontal axis (rising to right). The T-R points (empty squares in picture) represents the individual transgression/regression levels which were calculated from horizontal shift of the carbonate facies. At a rough estimate, 20m-change of sea level corresponds to one T-R unit in the diagram (sea level is rising towards the positive values). Bold asterisk marks the beginning of the eustatic curve in detail (Fig. 4). Connection of mean values has been used for better visualisation. But note that number of analysed components is limited, i.e. eventual omission of any of the components can change this curve significantly

value of -6.2 ‰; the difference between both $\delta^{13}C$ values is negligible (Tab. 1). Decreasing in $\delta^{18}O$ could be a result of increased ratio water/carbonate during pore water reactions or increased temperature, or as a simple result of diagenesis in the vadose zone (meteoric water). The later possibility seems to be supported by high content of Fe measured in a sample 2061 (Tab. 1).

The data for diagenetical cements in the HV-105 are scattered (Tab. 1). The samples represent stromatactis and mosaic sparite in the fractured nodules from the Famennian limestone and mosaic sparite in veins from the Early Frasnian limestone. The $\delta^{13}C$ values ranges from 1.8 to 2.6 ‰ and the $\delta^{18}O$ values ranges from -4.7 to -3.6 ‰ PDB.

## Diagenesis

Based on observations in thin sections, the structure and composition of the rock were little changed during the early stages of the diagenesis. There are only two exceptions for the levels where the platform (reef) margin matches the vertical section of the borehole, i.e. on its transgressional and regressional trajectory. The grainstone/rudstone of the reef margin or reef cap displays thin rims of the marine fibral cement whereas the scalenohedric, so-called dog-teeth cements are rare. Remnant porosity cavities are filled exclusively by mosaic sparite which possesses calcite crystals of medium dimensions. Zonality of the crystals in this mosaic sparite is very slight.

But majority of the sediments are packstones, both of lagoonal or fore-reef origin. These rocks are characterised by an abundance of micrite. Grains of micrite were nuclei of the crystal growth. However, this progressive recrystallisation by growth of micrite grains was accompanied by emergence of bunches of microscopic seams. Owing to abundance of micrite, the compactite types dominate the rock fabric. This feature of dissolution enabled rapid decrease in porosity which appeared already during the burial under the first tens to hundreds of meters of the sediment. Although the microstructures of the bioclasts, or any other details in particles and cements, are recognisable in details, their preservation in the rock corresponds exclusively to the positions of mineral inclusions and crystal defects ("shadows"). They are not represented by adequate crystal individuals. This preservation by means of the above mentioned "shadows" was caused by strong penetrative recrystallisation. A progressive mosaic overprint originated in places where the channel or intergranular/seam exchange of the fluids was still effective. On the other hand, about 75 % of the drilled thickness, were not changed significantly by this progressive recrystallisation. The next step of the recrystallisation is a very uniform, overall pervading recrystallisation which resulted in very fine aggregate of calcite crystals. Crystal size in this uniform aggregate fluctuate between 25-45 μm. The relationships to history of magnetite, as well as organic matter and colour alteration of conodonts, corroborate our assumption that the above mentioned degradation in crystal size originated in deep burial conditions, where the permeability of the rock was very low, but the temperature was high (about 350 °C; Krs et al. 1995). Thus, the structural homogenisation by the latter crystalline overprint is parallel to the documented overprints in magnetics, chemistry, and isotope compositions. Insufficiency of water in this "hot" alteration of the carbonate makes it difficult to explain the observed trend to homogenisation in structures and composition. Another possible alternative could be a hypothetical existence of low-rate diffusion, which influenced rock spots of metres dimensions (cf. Reeder 1983). However, this diffusion is still neither modelled nor documented in these dimensions.

In comparison with large data sets published by Veizer et al. (1986) or Carpenter and Lohmann (1989), the carbon and oxygen isotopic composition of most fossils and matrix from the HV-105 are in the range which is typical for

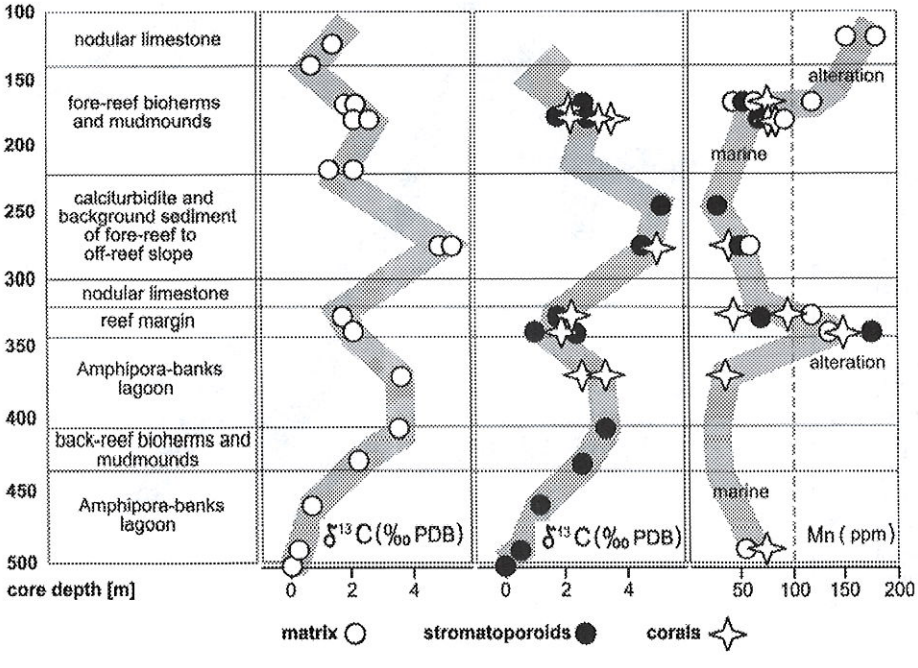


Fig. 7. The $\delta^{13}C$ data and Mn content. The decrease in the $\delta^{13}C$ values accompanied by the increase in Mn contents has been documented two times: first at the intersection of the well-log vertical and trajectory of the transgressively climbing reef margin (334.8 to 342.3 m), second at the intersection of the log and trajectory of the regressive backstepping of very late and extinct reef (124.5 to 178.4 m). These marginal reef facies were influenced by occasional emergence and vadose diagenesis. Trends in the $\delta^{13}C$ ratios are segmented by boundaries of the main facies in the HV-105 (left)

the Devonian marine carbonates. Nevertheless, the isotope composition of the limestone rock components in the HV-105 documents that the original mineralogical and isotope composition of rock components had to be partly changed (cf. the chapters about the fossils, matrix and cement). Thus, the recent isotope composition reflects the conditions, in which the metastable carbonates were stabilised. Considering the low contents of Mn and Fe, the lack of correlation between $\delta^{18}O$ values and Mn content, we suppose that stabilisation processes of the metastable carbonate phases took place during the early diagenetical, marine pore-water stages.

The lack of correlation between the isotopic and chemical data from the HV-105 corroborates the existence of closed systems where the diagenesis took place (Figs. 5 to 7). The isotopic and chemical composition of the HV-105 limestones document that these closed systems were disjoined into "cells" of different size. Of course, the boundaries of these cells are fuzzy. The vertical dimension of these "cells" varies from 0.5 to 10 m; in 3-D; they form probably the bedding-parallel spots and lenses (estimates of the elongation ratio ~ 1.5 to 10). These "cells" conserved almost the primary average isotopic composition which originated due to exchange among the formerly different components and which was formerly influenced by remnant pore water where marine bicarbonate prevailed.

In the HV-105, the isotopic composition of the cements from voids and fissures is very similar to overall values of the "cells". Any indication for the isotope exchange between the oxygen of carbonates and hot pore waters during the late stages of the diagenesis is absent. Thus, the rapid decrease in permeability happened before the maximum of the Variscan heating. This decrease in permeability was caused primarily by heavy supply of micrite and intensive lithification by blue-green algae, but the pronounced decrease in permeability had relation to the origin of "cells" which originated in burial conditions under the Viséan Culm deposits. During the Viséan, the diastrophic flysh formations covered the sinking carbonate complex in the continental slope and foot environment (aprx. 340 Ma). Of course, the heating alteration had to be effective still during the Westfalian when the tectonic "sandwich" structures were deformed by the Moravian Shear Zone (aprx. 310 Ma).

## Variation of $\delta^{13}C$ values at the basinal margin of the reef facies

As described above, the $\delta^{13}C$ values of carbonates from the HV-105 (0 to +5.5 ‰) are in the range of the typical marine sediments (cf. also Keith - Weber 1964). The $\delta^{13}C$ values measured within any of the selected depths ("cells") are similar, whereas the different "cells" provided different, cellular-specific values. The $\delta^{13}C$ values from 2 to 2.5 ‰ are characteristic for bioherms, deeper parts of the fore-reef to off-reef slope, and off-shore lagoons.

The minimum values (about 0 ‰) were documented in shallow back reef sediments. The isotopically light $CO_2$ may be ascribed either to continental or intensive photosynthetic sources (green-algae grass which was suppressing the amphiporid grass). However, the low contents of Mn, Fe, and siliciclastic clasts document that terrestrial shore was fairly away from this sedimentary environment. The situation of the reef margin is different. On this elevated reef margin, the $\delta^{13}C$ values are also low, but the Mn and Fe contents are increased. This suggests, together with sedimentology (light colour, brecciated structure, vadose silt), that the reef-edge elevation was in close touch with the sea-level. This edge was occasionally emerged even during the low-scale sea-level falls.

The highest, for marine environment anomalous $\delta^{13}C$ values were found in the fore reef (up to +5.5 ‰; cf. Tab. 1, Figs. 5 to 7). With the exception the $CO_2$ production related to decomposition of organic matter by methanogenetic bacteria, no other processes related to burial or meteoric diagenesis would produce a significant enrichment in $^{13}C$ (Lohmann 1988). Of course, the low content of the organic carbon in the rock (aprx. <0.1 %) does not corroborate an assumption about intensive methanogenesis. Consequently, the documented $\delta^{13}C$ anomaly is related to the original sedimentary conditions. From the view of facies, this anomaly is placed at the transition between the proximal and distal fore reef, just before the maximum peak of the transgression (sea level rise), in the time, when very steep gradient of sea-level rise was decreased. From the view of stratigraphy, this anomaly has been approximately correlated with the time interval of the conodont zone *Pa. transitans* (= formerly in the upper part of the Lower *Po. asymmetricus* Zone, i.e. by means of very rough time calibration between 371.0 and 371.4 Ma).

This anomalous isotopic composition which has been found in black sediments of the HV-105 fore reef differs from the majority of the published data. For example, Brand (1989) concluded from his studies on the North American and Eurasian Devonian brachiopods that the Early - Givetian (aprx. 378-380 Ma) and Frasnian /Famennian - boundary (aprx. 367 Ma) $\delta^{13}C$ values are about 3-4 ‰ PDB, whereas the Middle Givetian (aprx. 377-375 Ma) and Early Famennian (367-363 Ma) are characterised by the $\delta^{13}C$ values about 2-3 ‰ lower than in the adjacent periods. Carpenter - Lohman (1989) documented the $\delta^{13}C$ values in early diagenetical cements from the mostly Early Frasnian Golden Spike and Nevis reefs, Alberta, and they have found the $\delta^{13}C$ values which usually are between 1 and 3.5 ‰ PDB (up to the conodont zone *Ancyrognathus triangularis*). Regarding that information on any time-controlled global anomaly in the *Pa. transitans* Zone does not exist, then $\delta^{13}C$ anomaly in the HV-105 borehole is probably a result of local conditions in facies.

The fact that $\delta^{13}C$ anomaly occurred when shelves were widely submerged does not support the commonly

used explanation that upwelling was caused by disturbances in ocean water stratification in relation to the origination of the mixed-ocean. This scenario is restricted almost exclusively to the strong lowstand of sea level. It works well later in the Devonian, during the Kellwasser crisis and entire lowstand interval from the Kellwasser times to the Famennian (cf. McGhee et al. 1986, Hladil et al. 1991, Halas et al. 1992), but this is not a case of the early Frasnian highstand. The triggering mechanism of this upwelling had to be different, although the effect could be similar: Based on sedimentological data we suggest that huge amounts of nutrients were supplied to the surface waters thus allowing for a tremendous bloom of marine biota. The expanded marine biota preferentially take up the $^{12}C$ isotope and inevitably cause a rise in $^{13}C$ of bicarbonate. We can suggest a tentative scenario for the Moravian Karst off-shore which is based on the sedimentological data: The effect of a strong contour current has been documented at the frontal margin of the Late Givetian reefs (Isaacson - Galle 1991). This contour current which was born upon the Moravian Karst fore-reef slope was characteristic for both Late Givetian and earliest Frasnian. This current, when correction for the palaeomagnetically documented rotation is applied (120° clockwise; Krs et al. 1995), was oriented towards 80° ENE. However, the orientation of this current was just opposite to the surface, wind-driven current (270-290° WNW) which was responsible for the stratigraphically climbing migration routes of the Frasnian tabulate corals from Moravia to northern Rhenish Slate Mts. and Belgium (*Alveolites delhayei*, *Al. suborbicularis*). Later in the Frasnian, there is no evidence for this contour current. The trajectory of the east-directed contour current had to be significantly deflected towards the Devonian South. Simultaneously, the surface west-directed current also ceased, because the Middle to Late Frasnian continuation of this route was strongly reduced. Diversion of both currents, i.e. the surface wind-driven and contour current, and their reorientation towards the interiors of the Rhenish Basin (= from the Laurussian continent towards sea, in average) affected the circulation pattern. Two possible reasons exist for this change: the first explanation may be an analogy of Ekman transport which is typical for the contact between two atmospheric/hydrospheric circulation belts, the second explanation may be based on the changed morphology of islands or gates on the Devonian West and East. The both mechanisms involve the diversion of the currents and opening of a window in water stratification. These mechanisms result in the upwelling spots of the III$^{rd}$ category (cf. Wilde et al. 1990). In addition, the transtensional tectonism of the Rhenish back-arc basin, deltas of the Laurussian continent and local restrictions of bays could cause some subordinated disturbances, generating an unstable patchy pattern of water with different salinity and temperature. However, any consistent interpretation of the latter factors is still impossible due to discontinuity and scarcity of the data.

## Conclusions

1. Both $\delta^{13}C$ and $\delta^{18}O$ values of the Late Devonian limestones from the Křtiny HV-105 borehole are in the range typical for the Late Devonian marine and early diagenetic conditions.
2. No significant differences in chemical and carbon isotopic composition were found among fossil organic skeletons, matrix and other rock components.
3. Homogenisation in the C and O isotope contents originated in closed pore-water/rock systems, under conditions of rapidly decreased permeability. This type of changes corroborates the drowning of the fossil reef complex with a subsequent burial under a siliciclastic complex of Culm rocks.
4. Thus, the values from individual "cells" still involve significant information which is related to original facies. The $\delta^{13}C$ values of 2 to 2.5 ‰ are characteristic for bioherms, parts of the fore-reef to off-reef slope, and off-shore lagoons. The minimum values (about 0 ‰) are characteristic for shallow back-reef as an effect of algal grass. The low $\delta^{13}C$ values of reef margin developed during occasional emergence of this facies as documented by sedimentology and increased contents of Mn and Fe.
5. A significant anomaly in $\delta^{13}C$ values (up to +5.5 ‰) has been documented in the fore reef facies. This anomaly was found at the transition between the proximal and distal forereef. From the point of view of sea level changes, the $\delta^{13}C$ anomaly preceded the turnpoint to regression. The age of the anomaly has been correlated to the time interval of the conodont zone *Pa. transitans* (formerly in the upper part of the Lower *Po. asymmetricus* Zone). This anomaly of high $\delta^{13}C$ values do not correspond to global-event anomalies. It differs from the global isotope anomalies in age and intensity.
6. The existence of $\delta^{13}C$ anomaly in the slope of the Moravian Karst reefs cannot be explained by simple upwelling under conditions of lowstand and mixed ocean water. The upwelling effect had to be related to local features of the IIIrd category. The necessary window was formed by diversion of two sea currents, which were the deeper contour current and shallower wind-driven current.
7. The isotopic data from the HV-105 Křtiny borehole support our hypothesis that the facies control of the $\delta^{13}C$ values could be at least as strong as the global control based on oscillating oceanic carbon chemistry.

*Acknowledgement.* We thank to the Czech Geological Survey, Geological Institute (Academy of Sciences of the Czech Republic), and shareholders' cement company CEMO a.s. for systematic support of the studies of the Moravian Karst. This study was finalised within the IGCP Project 386 "Response of the Ocean/Atmosphere System to Past Global Changes". The authors appreciate chemical

analyses by M. Huka and M. Mikšovský and consultation of selected tasks of conodont and event stratigraphy by Z. Krejčí and J. Kalvoda. We thank for critical reading of the paper to K. Žák, I. Chlupáč and M. Novák.

*Submitted November 11, 1996*

## References

*Baker, P. A. - Gieskes, J. M. - Elderfield, H.* (1982): Diagenesis of carbonates in deep-sea sediments. - Evidence from Sr/Ca ratios and interstitial dissolved $Sr^{2+}$ data. - J. sed. Petrology, 52, 71-82. Lawrence.

*Brand, U.* (1981): Mineralogy and chemistry of the Lower Pennsylvanian Kedrick fauna, Eastern Kentucky. - Chem. Geol., 32, 17-28. Lawrence.

- (1989): Global climatic changes during the Devonian-Mississippian: Stable isotope biogeochemistry of brachiopods. - Palaeogeogr. Palaeoclimatol. Palaeoecol. (Global and Planetary Change Section), 75, 311-329. Amsterdam.

*Brand, U. - Veizer, J.* (1981): Chemical diagenesis of multicomponent carbonate system - 2: Stable isotope. - J. sed. Petrology, 51, 987-997. Lawrence.

*Carpenter, S. J. - Lohmann, K. C.* (1989): $\partial^{18}O$ and $\partial^{13}C$ variations in Late Devonian marine cements from the Golden Spike and Nevis Reefs, Alberta, Canada. - J. sed. Petrology, 59, 792-814. Lawrence.

*Carpenter, S. J. - Lohmann, K. C. - Holden, P. - Walter, L. M. - Huston, T. J. - Halliday, A. N.* (1991): $\partial^{18}O$, $^{87}Sr/^{86}Sr$ and Sr/Mg ratios of Late Devonian abiotic marine calcite: Implication for the composition of ancient seawater. - Geochim. cosmochim. Acta, 55, 1991-2010. Oxford.

*Crick, R. E.* (1996): Changes to the Geological Time Scale. Editorial Notes. - Subcommission on Devonian Stratigraphy Newsletter, 13, 1-2. Arlington.

*Crick, R. E. - Ellwood, B. - El Hassani, A.* (1994): Integration of Biostratigraphy, Magnetic Susceptibility, & Relative Sea-Level Change: A New Look at High Resolution Correlation. - Subcommission on Devonian Stratigraphy Newsletter, 11, 59-66. Arlington.

*Dvořák, J. - Friáková, O. - Galle, A. - Hladil, J. - Skoček, V.* (1984): Correlation of the reef and basin facies of Frasnian age in the Křtiny HV-105 borehole in the Moravian Karst. - Sbor. geol. Věd, Geol., 39, 73-103. Praha.

*Fordham, B. G.* (1992): Chronometric calibration of Mid-Ordovician to Tournaisian conodont zones: a compilation from recent graphic-correlation and isotope studies. - Geol. Mag., 129, 6, 709-721. London.

*Geldsetzer, H. H. J.* (1988): Ancient Wall reef complex, Frasnian age, Alberta. *In: H. H. J. Geldsetzer - N. P. James - G. E. Tebbutt* (eds): Reefs, Canada and adjacent areas. Canadian Society of Petroleum Geologists, Memoir, 13, 431-439. Calgary.

*Gradstein, F. M. - Ogg, J.* (1996): A Phanerozoic time scale. - Episodes, 19, 1-2, 3-5. Ottawa.

*Halas, S. - Balinski, A. - Gruszcynski, M. - Hoffman, A. - Malkowski, K. - Narkiewicz, M.* (1992): Stable isotope record at the Frasnian/Famennian boundary in southern Poland. - Neu. Jb. Geol. Paläont., Mh., 129-138. Stuttgart.

*Harland, W. B.* (ed.) (1990): A geologic time scale 1989. Cambridge University Press, 265 pp. Cambridge.

*Hedinger, A. S. - Workum, R. H.* (1988): Hummingbird and Whiterabbit reef margins (Frasnian), Alberta. *In: H. H. J. Geldsetzer - N. P. James - G. E. Tebbutt* (eds): Reefs, Canada and adjacent areas. Canadian Society of Petroleum Geologists, Memoir, 13, 457-460. Calgary.

*Hladil, J.* (1983): The biofacies section of Devonian limestones in the central part of the Moravian Karst. - Sbor. geol. Věd, Geol., 38, 71-94. Praha.

- (1988): Structure and microfacies of the Middle and Upper Devonian carbonate buildups in Moravia, Czechoslovakia. *In: N. J. McMillan - A. F. Embry - D. J. Glass* (eds.): Devonian of the World, II, Canad. Soc. Petrol. Geol. Mem., 4, 2, 607-618. Calgary.

*Hladil, J. - Kalvoda, J.* (1993): Life strategies during the extinction and recovery at Eifelian-Givetian and Frasnian-Famennian boundaries in Bohemia and Moravia. - Global Boundary Events, Kielce 1993. Abstracts: 22. Kielce.

*Hladil, J. - Krejčí, Z. - Kalvoda, J. - Ginter, M. - Galle, A. - Beroušek, P.* (1991): Carbonate ramp environment of Kellwasser time-interval (Lesní lom, Moravia, Czechoslovakia). - Bull. Soc. belg. Géol., 100, 1-2, 57-119. Bruxelles.

*Holser, T. - Magaritz, M. - Ripperdan, R. L.* (1995): Global Isotopic Events. *In: O. H. Wallise*: Global Events and Event Stratigraphy in the Phanerozoic, 63-88. Springer Verlag. Berlin.

*Hudson, J. D.* (1977): Stable isotopes and limestone lithification. - J. Geol. Soc., 133, 637-660. London.

*Isaacson, P. E. - Galle, A.* (1991): Significance of Amphipora floatstones within the Lažánky Limestone (Late Givetian), Moravian Karst. - Věst. Ústř. Úst. geol., 66, 5, 275-285. Praha.

*Joachimski, M. M. - Buggisch, W.* (1992): Carbon Isotope Shifts at the Frasnian/Famennian Boundary: Evidence for Worldwide Kellwasser Events? - Fifth International Conference on Global Bioevents, Göttingen, February 16-19, 1992. Abstract Vol., 58-59. Göttingen.

- (1993): Anoxic events in the late Frasnian - Causes of the Frasnian-Famennian faunal crisis? - Geology, 21, 675-678. Boulder.

*Jux, U. - Manze, U.* (1976): Milieu-Indikatoren aus einem biostromalen Riff des Bergischen Landes mittels C-Isotopen. - Decheniana, 129, 245-262. Bonn.

*Jux, U. - Zygojanis, N.* (1983): Kohlenwasserstoffgehalte und isotopische Zusammensatzung oberdevonischer Karbonatgesteine (Oberer Plattenkalk) der Bergisch Gladbach - Paffrather Mulde (Bergisches Land). - Neu. Jb. Geol. Paläont., Abh., 167, 1, 89-131. Stuttgart.

*Keith, M. L. - Weber, J. N.* (1964): Isotopic composition and environmental classification of selected limestones and fossils. - Geochim. cosmochim. Acta, 28, 1787-1816. Oxford.

*Krhovský, J. - Čejchan, P.* (1995): Cascade of causally linked effects of rapid glaciation-deglaciation events: a possible cause of non-selectivity of mass extinctions. *In: P. Čejchan - J. Hladil - P. Štorch* (eds): Evolution and extinctions. Proceedings of the Second Local Meeting of the IGCP 335 Project "Recoveries from mass extinctions". - Geolines, 3, 27-37. Praha.

*Krs, M. - Hladil, J. - Krsová, M. - Pruner, P.* (1995): Palaeomagnetic evidence for Variscan palaeotectonic rotation of Moravian Devonian rocks (in Czech). - Geol. Výzk. Mor. Slez. v Roce 1994, 2, 53-57. Brno.

*Lohmann, K. C.* (1988): Geochemical patterns of meteoric diagenetic systems and their application to studies of palaeokarst. *In: N. P. James - P. W.Choquette* (eds.): Palaeokarst. 58-80. Springer Verlag. Berlin, New York.

*May, A.* (1995): Relationship among sea-level fluctuation, biogeography and bioevents of the Devonian: an attempt to approach a powerful, but simple model for complex long-range control of biotic crises. *In: P. Čejchan - J. Hladil - P. Štorch* (eds): Evolution and extinctions. Proceedings of the Second Local Meeting of the IGCP 335 Project "Recoveries from mass extinctions". - Geolines, 3, 38-49. Praha.

*McConnaughey, T.* (1989): $^{13}C$ and $^{18}O$ isotopic disequilibrium in biological carbonates: II. in vitro simulation of kinetic isotope effects. - Geochim. cosmochim. Acta, 53, 163-171. Oxford.

*McCrea, J. M.* (1950): On the isotope chemistry of catbonates and palaeotemperature scale. - J. phys. Chem., 18, 649-657. Lancaster.

*McGhee, G. R. Jr. - Orth, Ch. J. - Quintana, L. R. - Gilmore, J. S. - Olsen, E. J.* (1986): Geochemical analyses of the late Devonian Kellwasser Event stratigraphic horizon at Steinbruch Schmidt (F.R.G.). *In: O. H. Walliser* (ed.): Global Bio-Events, Lecture Notes in Earth Sciences, 8, 219-224. Springer Verlag. Berlin.

*Milliman J. D.* (1974): Marine carbonates. - Springer Verlag. Berlin.

*Mistiaen, B.* (1984): Disparition des Stromatopores paléozoiques ou survie du groupe: hypothése et discussion. - Bull. Soc. géol. France, 7, 26, 6, 1245-1250. Paris.

*Morrow, J. R. - Schindler, E. - Walliser, O.H.* (1995): Phanerozoic Development of Selected Global Environmental Features. *In: O. H. Walliser*: Global Events and Event Stratigraphy in the Phanerozoic, 53-62. Springer Verlag. Berlin.

*Reeder, R. J.*, ed. (1983): Carbonates: Mineralogy and Geochemistry. - Mineral. Soc. Amer., Rev. Mineral., 11, 535 pp. Washington.

*Sansone, F. J. - Haberstroh, P. R.* (1995): Time-Series Measurements of Wave-Induced Porewater-Seawater Mixing in the Upper Framework of Coral Reefs. - Biology and Geology of Coral Reefs, September 5th to 9th 1995, European Meeting of the International Society for Reef Studies (ISRS) and the British Ecological Society (BES), Programme and Abstracts, University of Newcastle, Newcastle upon Tyne.

*Shen Jian-wei* (1995): Middle-Upper Devonian conodont succession and sea-level change in Guilin. - Acta micropalaeontol. sinica, 12, 3, 251-273. Beijing.

*Taraba, J.* (1976): Moravian Karst: regional survey of water resources (in Czech). - MS Geofond. Praha.

*Veizer, J. - Fritz, P. - Jones, B.* (1986): Geochemistry of brachiopods: Oxygen and carbon isotopic records of Palaeozoic oceans. - Geochim. cosmochim. Acta, 50, 1679-1696. Oxford.

*Walliser, O. H.* (1995): Global Events in the Devonian and Carboniferous. *In: O. H. Walliser*: Global Events and Event Stratigraphy in the Phanerozoic, 225-250. Springer Verlag. Berlin.

*Wanless, H. R. - Tedesco, L. P.* (1993): Depositional and Early Diagenetic Controls on Texture and Fabric of Carbonate Mudbanks, South Florida. *In: R. Rezak, - D. L. Lavoie* (eds): Carbonate Microfabrics. Frontiers in Sedimentary Geology, 41-64. Springer Verlag. Berlin.

*Wilde, P. - Quinby-Hunt, M. S. - Berry, W. B. N.* (1990): Vertical Advection from Oxic or Anoxic Water from the Main Pycnocline as a Cause of Rapid Extinction or Rapid Radiations. *In: E. G. Kauffman - O. H. Walliser* (eds): Extinction Events in Earth History, Lecture Notes in Earth Sciences, 30, 85-98. Springer Verlag. Berlin.

*Zorn, H.* (1977): Zur Skeletstruktur und Mineralogie devonischer und triassischer Korallen und anderer Rifforganismen. - Neu. Jb. Geol. Paläont., Mh., 6, 343-357. Stuttgart.

## Rozlišení faciálních a globálních změn v izotopovém složení karbonátů: izotopy uhlíku a kyslíku na čelním okraji devonského útesového komplexu na Moravě (vrt Křtiny HV-105)

Hodnoty $\delta^{13}C$ a $\delta^{18}O$ zjištěné v materiálu z vrtu Křtiny HV-105 spadají do rozmezí, které charakterizuje mořské a časně diagenetické prostředí mladšího devonu. Mezi zkamenělými zbytky karbonátových koster organizmů, různými typy horninové základní hmoty a tmely nebyly v izotopovém složení zjištěny výrazné rozdíly. Původní izotopické složení fosilií a horninových karbonátových komponent bylo částečně změněno v uzavřených systémech pórové vody a horniny, za podmínek prudce snížené propustnosti, avšak ještě při diagenezi v pórové vodě mořského složení. Takový typ změn dokládá klesání zaniklého útesového komplexu a jeho následné pohřbení pod siliciklastický komplex kulmských hornin. Hodnoty $\delta^{13}C$ od 2,0 do 2,5 ‰ jsou charakteristické pro biohermy, část prostoru před útesovým okrajem až odlehlých pánevních prostor a laguny vzdálené od pobřeží. Nejnižší hodnoty $\delta^{13}C$ (blízké 0 ‰) jsou charakteristické pro mělké části karbonátové plošiny za útesem a za svůj vznik vděčí řasovým "trávníkovým porostům". Nízké hodnoty $\delta^{13}C$ z čelní hrany útesového komplexu vznikly během příležitostného vynořování této facie, což je doloženo na základě sedimentologických znaků a zvýšeného obsahu Mn a Fe. Významná anomálie $\delta^{13}C$ (až +5.5 ‰) byla nalezena v části prostoru před útesem. Nalézá se na přechodu mezi horní a spodní částí čelního svahu útesového komplexu, z časového hlediska pak právě před dosažením maxima relativního zdvihu mořské hladiny. Stáří anomálie je přibližně určeno jako ekvivalent konodontové zóny *Pa. transitans* (řazené dříve do vyšší části zóny spodní *Po. asymmetricus*). Neobvyklé zvýšení obsahu izotopu $^{13}C$ se vymyká popisu anomálií spojených s globálními eventy. Existenci této anomálie na svahu útesů Moravského krasu nelze proto vysvětlit jednoduchým výstupem hlubokých mořských vod za podmínek významného snížení mořské hladiny a vznikajícího vertikálního mísení vod oceánů a moří. Výstup hlubších vod bohatých živinami a způsobující obrovský rozkvět fytoplanktonu v horních vrstvách moře musí být vztahován k místním jevům tzv. třetí kategorie. Nezbytné okno pro výstup hlubších vod bylo vytvořeno odkloněním dvou proudů od pobřeží Moravského krasu: jednak hlouběji položeného konturového proudu, jednak větrem hnaného povrchového proudu. Údaje z vrtu HV-105 Křtiny podporují hypotézu, že faciální vlivy mohou mít stejně silný účinek na výskyt anomálních hodnot $\delta^{13}C$ jako globální řízení obsahu izotopu $^{13}C$ v sedimentu měnícím se poměrem izotopů uhlíku ve vodách světových moří.